Many-body symmetry-adapted perturbation theory of intermolecular interactions. H_2O and HF dimers

Stanisl/aw RybakBogumil/ JeziorskiKrzysztof Szalewicz

Citation: The Journal of Chemical Physics **95**, 6576 (1991); doi: 10.1063/1.461528
View online: http://dx.doi.org/10.1063/1.461528
View Table of Contents: http://aip.scitation.org/toc/jcp/95/9
Published by the American Institute of Physics

Many-body symmetry-adapted perturbation theory of intermolecular interactions. H_2O and HF dimers

Stanisław Rybak
Institute of Chemistry, University of Warsaw, al. Pilsudskiego 11/4, 15-443 Bialystok, Poland and Department of Physics and Astronomy, University of Delaware, Newark, Delaware 19716

Bogumił Jeziorski
Department of Chemistry, University of Warsaw, ul. Pasteura 1, 02-093 Warsaw, Poland and Department of Physics and Astronomy, University of Delaware, Newark, Delaware 19716

Krzysztof Szalewicz
Department of Physics and Astronomy, University of Delaware, Newark, Delaware 19716

(Received 18 October 1990; accepted 16 July 1991)

A many-body version of the symmetry-adapted perturbation theory is developed for a direct calculation of intermolecular potentials as a sum of the electrostatic, exchange, induction, and dispersion contributions. Since no multipole expansion is used, the obtained interaction energy components are properly dampened at short distance by the charge-overlap (penetration) effects. The influence of the intramonomer correlation is accounted for by the perturbation expansion in terms of the Møller–Plesset type fluctuation potentials W_A and W_B for the individual molecules. For the electrostatic and for the dispersion energy, the terms of the zeroth, first, and second order in $W_A + W_B$ are considered. In this way, the leading three-particle correlation contribution to the dispersion energy is taken into account. As a test of our method, we have performed calculations of the interaction energy for the water and hydrogen fluoride dimers. Both the geometry and the basis set dependence of the interaction energy components have been investigated. For a comparison, we have also computed the supermolecular interaction energies through the full fourth order of the many-body perturbation theory. On the basis of our results, we predict the association energy for $(H_2O)_2$ equal to -4.7 ± 0.2 kcal/mol in relatively poor agreement with the experimental value of -5.4 ± 0.7 kcal/mol, but still within the experimental error bars. For $(HF)_2$, the predicted association energy is -4.2 ± 0.2 kcal/mol, while the experimental value (corrected by a theoretical zero-point energy) is -4.9 ± 0.1 kcal/mol.

I. INTRODUCTION

Weak interactions between closed-shell atoms and molecules play an important role in a great variety of physical and chemical phenomena. These interactions are also essential for a molecular-level understanding of biochemical processes, which are often initiated by the van der Waals interactions and/or by the hydrogen bond formation. Since a direct experimental determination of intermolecular potentials is either very difficult or at present impossible, one has to rely on theoretical calculations to obtain detailed information about radial and angular dependencies of the interaction energy. However, despite considerable progress made recently in this field, a reliable *ab initio* prediction of interaction potentials is still a highly nontrivial task even for small atoms and molecules.[1,2]

The *ab initio* methods used to calculate the interaction energy can be classified as *supermolecular*, *perturbational*, and *hybrid* ones. In a *supermolecular* method, the interaction energy is defined as

$$\tilde{E}_{\rm int} = \tilde{E}_{AB} - (\tilde{E}_A + \tilde{E}_B), \tag{1}$$

where $\tilde{E}_A$, $\tilde{E}_B$, and $\tilde{E}_{AB}$ are approximations to the exact ground-state energies E_A, E_B, and E_{AB} of the monomers A, B, and of the complex AB, respectively. These approximate energies can be computed using any method of solving the clamped-nuclei Schrödinger equation. For typical interactions of closed-shell systems, the exact interaction energy $E_{\rm int} = E_{AB} - (E_A + E_B)$ is from four to seven orders of magnitude smaller than the total energies E_A, E_B, and E_{AB}. Since even with the present supercomputer capabilities the errors $E_{AB} - \tilde{E}_{AB}$, $E_A - \tilde{E}_A$, and $E_B - \tilde{E}_B$ are always much larger than the interaction energy itself, $\tilde{E}_{\rm int}$ can be a good approximation to $E_{\rm int}$ only if a fortunate cancellation of these large errors occurs. For certain approximate methods, such a cancellation apparently takes place, although this fact has never been proven *a priori* in a convincing way. There are some necessary (although not sufficient) conditions which a supermolecular approach has to fulfill to provide a reasonable description of the intermolecular interaction: (i) the method has to be extensive and size consistent;[3] (ii) it has to account for the electron correlation sufficiently well; and (iii) the approximate monomer energies $\tilde{E}_A$ and $\tilde{E}_B$ have to be calculated using the full orbital basis of the complex AB, i.e., the so-called *basis set superposition error* must be eliminated.[4–11]

Perturbational methods compute the interaction energy $E_{\rm int}$ directly (i.e., no subtraction of much larger quantities is involved) as a sum of physically distinct contributions

$$E_{\rm int} = E^{(1)}_{\rm pol} + E^{(1)}_{\rm exch} + E^{(2)}_{\rm pol} + E^{(2)}_{\rm exch} + \cdots, \tag{2}$$

where $E^{(1)}_{\rm pol}$ is the classical electrostatic interaction energy, $E^{(2)}_{\rm pol}$ is a sum of the classical induction and quantum mechanical dispersion energies

 0021-9606/91/216576-26$03.00

$$E_{\rm pol}^{(2)} = E_{\rm ind}^{(2)} + E_{\rm disp}^{(2)}, \tag{3}$$

and $E_{\rm exch}^{(n)}$, $n = 1,2$ are exchange corrections defined by the symmetry-adapted perturbation theory (SAPT).[12,13] The exchange corrections can be physically interpreted as an effect of the resonance tunneling of electrons between interacting systems. In the perturbational methods, the clamped nuclei Hamiltonian H for the complex AB is divided into the unperturbed operator H_0 being the sum of the Hamiltonians for molecules A and B, i.e., $H_0 = H_A + H_B$, and the interaction operator V defined as the difference $V = H - H_0$. The polarization corrections $E_{\rm pol}^{(n)}$ are the coefficients in the Taylor expansion of the ground-state eigenvalue $E(\zeta)$ of the Hamiltonian $H(\zeta) = H_0 + \zeta V$, i.e., these corrections are identical with the Rayleigh–Schrödinger (RS) perturbation energies corresponding to the partitioning $H = H_0 + V$. Since the RS method completely neglects the exchange of electrons, it is called, after Hirschfelder,[14] the *polarization expansion*. In this theory, V is *not* expressed in terms of the multipole expansion,[15] therefore the damping effect of the penetration (the charge overlap) is properly taken into account. Thus, the polarization energies $E_{\rm pol}^{(n)}$ have a well-defined meaning for all intermolecular distances.

It should be noted that the exchange corrections $E_{\rm exch}^{(n)}$ obtained in SAPT are not unique for $n > 1$. Different formulations of SAPT[13,16–20] lead to different expressions for $E_{\rm exch}^{(n)}$ and, consequently, to different convergence rates of the expansion (2).[21–24] For the van der Waals interactions of nonpolar and weakly polarizable systems, the differences between various SAPT expansions are not important because the interaction energy is dominated by the first three terms in the expansion (2) and, moreover, the second-order exchange energies in various SAPT schemes do not differ significantly. However, for polar and strongly polarizable systems when appreciable charge transfer and exchange deformation can take place,[25,26] the induction part of $E_{\rm exch}^{(2)}$, i.e., the so-called exchange-induction energy,[27] as well as higher-order induction and exchange-deformation corrections are not negligible (exchange-deformation energy represents that part of the exchange energy which, unlike the exchange-induction energy, is not related to the polarization wave function). In those cases, the simplest version of SAPT may be slowly convergent. This difficulty can be circumvented by a *hybrid* approach to the calculation of $E_{\rm int}$. Since most of the exchange-induction and higher-order induction contribution is contained in the Hartree–Fock (HF) interaction energy $E_{\rm int}^{\rm HF}$,[24,26,28] one can perform a selective infinite-order summation of the series (2) and replace all the terms taken into account in the HF theory by $E_{\rm int}^{\rm HF}$. The resulting approximate expression for the interaction energy is

$$E_{\rm int} = E_{\rm int}^{\rm HF} + E_{\rm intra}^{(1)} + E_{\rm ind\text{-}intra}^{(2)} + E_{\rm disp}^{(2)} + E_{\rm exch\text{-}disp}^{(2)} + \cdots, \tag{4}$$

where $E_{\rm intra}^{(1)}$ collects the intramonomer correlation contribution to $E^{(1)}$, $E_{\rm ind\text{-}intra}^{(2)}$ represents analogous contributions to $E_{\rm ind}^{(2)}$, and $E_{\rm exch\text{-}disp}^{(2)}$ is the exchange-dispersion energy.[27] The latter contribution is a part of $E_{\rm exch}^{(2)}$ and represents an effect of the exchange damping of the dispersion interaction.

For molecules of the size of water $E_{\rm int}^{\rm HF}$ can presently be computed very accurately from Eq. (1) using the self-consistent field (SCF) orbital expansions. Therefore, the difficulties of the supermolecular approach discussed earlier can be well controlled at the Hartree–Fock level of theory. Since the major components of $E_{\rm int}^{\rm HF}$ are known from the perturbational analysis,[24,26,28] expression (4) still possesses a clear physical interpretation. The individual interaction energy components in the expansion (4) can be calculated independently using specifically designed methods and basis sets.[29] Equation (4) has also been used with great success for the construction of model van der Waals potentials.[30–34]

The present paper is devoted to the evaluation of the interaction energy components appearing in Eq. (2) or Eq. (4) for many-electron systems. (An initial account of this work has been presented in Ref. 35). Since neither the exact eigenfunctions of H_0, nor even some reasonable approximations to them can be computed in practice for any but two-electron molecules, one has to use the HF-SCF determinants as the starting point and apply some kind of perturbation theory to take account of the intramonomer electron correlation. The monomer Hamiltonians H_A and H_B are decomposed as $H_A = F_A + W_A$ and $H_B = F_B + W_B$, where F_A and F_B are the Fock operators for molecules A and B, respectively (the Møller–Plesset partitioning). Thus, the total Hamiltonian can be written as

$$H(\zeta,\xi,\eta) = F + \zeta V + \xi W_A + \eta W_B, \tag{5}$$

where $F = F_A + F_B$ and the formal expansion parameters ζ, ξ, and η have the physical value equal to unity. By applying a triple RS-type perturbation theory, one can derive a many-body expansion of the corrections $E_{\rm pol}^{(n)}$ in terms of the correlation operators (or fluctuation potentials) W_A and W_B of individual monomers

$$E_{\rm pol}^{(n)} = \sum_{i=0}^{\infty}\sum_{j=0}^{\infty} E_{\rm pol}^{(nij)}, \tag{6}$$

where $E_{\rm pol}^{(nij)}$ is of the nth order in V, of the ith order in W_A, and of the jth order in W_B. The corrections $E_{\rm pol}^{(nij)}$ are formally defined as the coefficients in the Taylor expansion of the ground-state eigenvalue $E(\zeta,\xi,\eta)$ of $H(\zeta,\xi,\eta)$. The expansion (6) and a similar expansion for the exchange components $E_{\rm exch}^{(n)}$ have been introduced in Refs. 36 and 37, but the general problem of expanding individual terms in Eq. (6) through one- and two-electron integrals (perturbation theory diagrams) has not been considered thus far. When the expansion (6) (and a similar expansion for $E_{\rm exch}^{(n)}$) is inserted into Eq. (2), one obtains a many-body SAPT expansion for the total interaction energy. The corrections $E_{\rm pol}^{(n00)}$ can be viewed as describing the interaction of "Hartree–Fock" molecules, while the remaining terms in the expansion (6) represent the intramonomer correlation effect.

The intramonomer correlation corrections are obviously more difficult to evaluate than the leading term $E^{(n00)}$ in Eq. (6). In the present paper we shall restrict our considerations to the intramonomer correlation contributions to the polarization energies only, while the analogous exchange corrections will be neglected. A derivation of a many-body expansion for the exchange energies presents a more difficult

problem because of the necessity to handle overlap integrals for nonorthogonal sets of orbitals. When the intramonomer correlation is neglected, this nonorthogonality is manageable and the problem was solved some time ago both in the case of the first-order exchange energy[38] $E^{(100)}_{exch}$ and the exchange-dispersion energy[39] $E^{(200)}_{exch\text{-}disp}$. Among all the intramonomer correlation contributions to the exchange energies, only the corrections of the first order in V can be expected to give a nonnegligible contribution. We are presently developing efficient methods of evaluating these corrections and an initial step in this direction has been reported in Ref. 40.

The plan of this paper is as follows: In Sec. II, we present a general formulation of the polarization expansion for the interaction energy based on the coupled-cluster (CC) form of the Schrödinger equation.[41–44] This formulation leads to the many-body theory in which only connected quantities appear and one does not have to perform explicitly cancellations of unlinked diagrams.[45] The leading intramonomer correlation contribution to the electrostatic energy is considered in Sec. III, while Sec. IV contains discussion of the many-body expansion of the dispersion energy. Section V gives the formulas for the leading-order exchange corrections in a form and notation consistent with the present

TABLE I. List of the SAPT corrections computed in this work. The perturbation theory is based on the partitioning of the total Hamiltonian as $H = F + V + W$, where the zeroth-order operator $F = F_A + F_B$ is the sum of the Fock operators for the monomers, the intermolecular potential $V = H - H_A - H_B$ is the difference between the Hamiltonians of interacting and noninteracting systems, and the fluctuation potential $W = W_A + W_B$ is the sum of the Møller–Plesset fluctuation potentials of the monomers $W_C = H_C - F_C$. All corrections include the damping due to the charge overlap effects. The superscripts n and l in a correction $E^{(nl)}$ denote the orders of perturbation in V and W, respectively.

Symbol	Equation number	Name	Physical interpretation
$E^{(10)}_{pol}$	(39)	Electrostatic energy	Describes electrostatic interactions of permanent electric multipole moments of the monomers (computed in the Hartree–Fock approximation).
$E^{(10)}_{exch}$	(105)	Exchange repulsion	Results from exchange of electrons (quantum mechanical tunneling) between interacting systems.
$E^{(12)}_{pol}$	(54)–(56)	Correlation correction to electrostatic energy	Describes electrostatic interactions of the correlated multipole moments of the monomer A with uncorrelated moments of the monomer B and vice versa (through the second order in W).
$E^{(20)}_{ind}$	(62)	Induction energy	Due to interactions between the permanent and induced multipole moments resulting from the polarization of the monomer A by the permanent multipole moments of the monomer B and vice versa.
$E^{(20)}_{disp}$	(63)	Dispersion energy	Resulting from quantum mechanical charge fluctuations (interactions of "induced instantaneous electric moments"); since this correction is of zeroth order in W, it can be called the dispersion interaction of "Hartree–Fock" atoms or molecules.
$E^{(20)}_{exch\text{-}disp}$	(108)–(110)	Exchange-dispersion energy	Due to the coupling of electron exchange to dispersion interaction in zeroth order with respect to W.
$E^{(21)}_{disp}$	(70)–(72)	Correlation correction to dispersion energy	Leading intramonomer correlation correction (of the first order in W). Describes coupling of the intramonomer correlation effects to intermolecular dispersion interaction.
$E^{(22)}_{disp}$	(80)–(82), (91)–(99), (101)	Correlation correction to dispersion energy	Second-order (in W) intramonomer correlation correction to dispersion energy.
$E^{(30)}_{disp}$	(103)	Third-order dispersion energy	Correction similar to $E^{(20)}_{disp}$, but of the third order with respect to V.

work. The theory presented in Secs. II–V is somewhat involved and we do not expect every reader interested in intermolecular interactions to be willing to study it in detail. To help understand the meaning of various contributions to the interaction energy, we present in Table I the list of all perturbation theory corrections considered in this work together with their physical interpretation and a reference to the equations defining them. This table should make it possible to skip Secs. III–V (and even Sec. II) and go directly to Sec. VI where we discuss the results of numerical calculations for $(H_2O)_2$ and $(HF)_2$. Section VII contains a general discussion and conclusions.

II. MANY-BODY POLARIZATION EXPANSION

The standard, generally accepted definitions of the dispersion energy $E^{(2)}_{\rm disp}$ and other polarization corrections involve *nonsymmetric* unperturbed operators $H_0 = H_A + H_B$ or $F = F_A + F_B$. These operators do not include all electrons in a fully symmetric way and, consequently, do not preserve the antisymmetry property of the wave functions upon which they act. Thus, H_0 and F are not legitimate operators in the conventional antisymmetric Hilbert space $\mathcal{H}$ for $N = N_A + N_B$ electrons (N_C, $C = A$ or B, is the number of electrons of the molecule C). To use these operators, we have to consider a larger space $\mathcal{H}_A \otimes \mathcal{H}_B$ being the tensor product of Hilbert spaces $\mathcal{H}_A$ and $\mathcal{H}_B$ for molecules A and B. The Hilbert spaces $\mathcal{H}_A$ and $\mathcal{H}_B$ are individually antisymmetric, i.e., they contain only antisymmetric functions of N_A and N_B electrons, respectively. Thus, $\mathcal{H}_A \otimes \mathcal{H}_B$ includes all functions of $N_A + N_B$ electronic coordinates which are antisymmetric with respect to permutations of electrons *within* each of the monomers. Permutations of electrons between interacting molecules will generally lead to wave functions not belonging to $\mathcal{H}_A \otimes \mathcal{H}_B$. However, one may prove that when the one-electron spaces used to construct $\mathcal{H}_A$ and $\mathcal{H}_B$ are complete, any antisymmetric function can be expanded in terms of products $\Psi_I\Psi_J$, $\Psi_I \in \mathcal{H}_A$, $\Psi_J \in \mathcal{H}_B$, and, consequently, $\mathcal{H} \subset \mathcal{H}_A \otimes \mathcal{H}_B$. Thus, in this case, all physical solutions of the Schrödinger equation belong to $\mathcal{H}_A \otimes \mathcal{H}_B$. This result holds also when the orbital bases are finite and incomplete (i.e., in the *algebraic approximation*) provided that the one-electron spaces used to construct $\mathcal{H}_A$ and $\mathcal{H}_B$ are identical. We shall always assume that this is the case, i.e., that the so-called *dimer-centered basis set* is used in calculations. If the *monomer-centered basis sets*[1,2] were used to construct $\mathcal{H}_A$ and $\mathcal{H}_B$, the antisymmetric functions would not belong to $\mathcal{H}_A \otimes \mathcal{H}_B$ and exchange effects would converge slowly. It should be pointed out that the dispersion energy $E^{(2)}_{\rm disp}$ cannot be defined using the fully antisymmetric Hilbert space $\mathcal{H}$ and the introduction of $\mathcal{H}_A \otimes \mathcal{H}_B$ is necessary.

A. Second-quantization formalism for nonsymmetric operators

To introduce an appropriate second-quantization formalism for nonsymmetric operators, we have to consider the generalized Fock space $\mathcal{F}_{AB} = \mathcal{F}_A \otimes \mathcal{F}_B$, where $\mathcal{F}_C$, $C = A$ or B is the usual Fock space for the electrons of the molecule C. The annihilation (creation) operators acting in $\mathcal{F}_A$ and $\mathcal{F}_B$ will be denoted by a_μ ($a^\dagger_\mu$) and b_μ ($b^\dagger_\mu$), respectively. These operators satisfy the following (anti)commutation relations:

$$\{a_\mu, a_\nu\} = \{b_\mu, b_\nu\} = \{a^\dagger_\mu, a^\dagger_\nu\} = \{b^\dagger_\mu, b^\dagger_\nu\} = 0, \tag{7}$$

$$\{a^\dagger_\mu, a_\nu\} = \{b^\dagger_\mu, b_\nu\} = \delta_{\mu\nu}, \tag{8}$$

$$[a_\mu, b_\nu] = [a^\dagger_\mu, b_\nu] = [a_\mu, b^\dagger_\nu] = [a^\dagger_\mu, b^\dagger_\nu] = 0, \tag{9}$$

where $[\,,\,]$ and $\{\,,\,\}$ denote the commutator and anticommutator, respectively. Equations (7) and (8) are a consequence of the orthonormality of the spin orbital basis set ϕ^A_μ (ϕ^B_μ) used to define a_μ (b_μ). Equation (9) results from the fact that the operators a_μ and b_μ act on differents sets of variables. This means that the electrons of molecules A and B are treated as different, *distinguishable* particles. This is not an approximation since the exact antisymmetric function Ψ can be expanded in terms of the product functions $\Psi_A\Psi_B \in \mathcal{H}_A \otimes \mathcal{H}_B$, so that the Schrödinger equation $H\Psi = E\Psi$ can still be fulfilled exactly in $\mathcal{F}_{AB}$. However, one should be aware of the fact that $\mathcal{F}_{AB}$ also contains solutions of the Schrödinger equations which do not correspond to any physical states of the complex AB since they do not satisfy the Pauli principle.

Using the creation and annihilation operators, one can write the operators F_C and W_C, $C = A$ or B in the following second-quantized form:

$$F_C = (f_C)^\mu_\nu c^\nu_\mu, \tag{10}$$

$$W_C = \tfrac{1}{4} w^{\lambda\kappa}_{\mu\nu} c^{\mu\nu}_{\lambda\kappa} - w^{\mu\gamma}_{\nu\gamma} c^\nu_\mu, \quad \gamma \in C, \tag{11}$$

where $(f_C)^\mu_\nu$ are the matrix elements of the Fock operator for molecule C, $w^{\lambda\kappa}_{\mu\nu}$ are the antisymmetrized two-electron integrals

$$w^{\lambda\kappa}_{\mu\nu} = \langle \phi_\mu(1)\phi_\nu(2) | r_{12}^{-1}(1 - P_{12})\phi_\lambda(1)\phi_\kappa(2) \rangle, \tag{12}$$

and the symbol $c^{\lambda\kappa\cdots}_{\mu\nu\cdots}$, $c = a$ or b denotes the product

$$c^{\lambda\kappa\cdots}_{\mu\nu\cdots} = c^\dagger_\lambda c^\dagger_\kappa \cdots c_\nu c_\mu. \tag{13}$$

Summation over repeated *lower* and *upper* indices is implied in Eqs. (10) and (11) and throughout the rest of this paper (the Einstein convention). We shall also always assume that $\alpha,\beta,\gamma,\delta$ (ρ,σ,τ,ω) label occupied (virtual) spinorbitals, while λ,κ,μ,ν are used when all spin orbitals (both occupied and unoccupied) can occur in a summation or in a formula. It will be clear from the context whether the indices λ,κ,μ,ν pertain to spin orbitals of molecule A or molecule B. However, we shall always assume that lower case Greek letters α and ρ (β and σ) label the spin orbitals of molecule A (molecule B). The intermolecular interaction operator V can be represented in the form

$$V = v^{\lambda\kappa}_{\mu\nu} a^\mu_\lambda b^\nu_\kappa + (v_A)^\lambda_\mu b^\mu_\lambda + (v_B)^\kappa_\nu a^\nu_\kappa + V_0, \tag{14}$$

where V_0 is the constant nuclear repulsion term,

$$v^{\lambda\kappa}_{\mu\nu} = \langle \phi_\mu(1)\phi_\nu(2) | r_{12}^{-1} | \phi_\lambda(1)\phi_\kappa(2) \rangle, \tag{15}$$

and $(v_C)^\nu_\mu = \langle \phi_\mu | v_C | \phi_\nu \rangle$ is a matrix element of the electrostatic potential

$$v_C(\mathbf{r}_i) = -\sum_{\alpha \in C} \frac{Z_\alpha}{r_{\alpha i}}, \tag{16}$$

of all the nuclei of molecule C. Z_α denotes here the charge of the αth nucleus and $r_{\alpha i}$ the distance of electron i from this nucleus.

Equations (10) and (11) are the standard expressions of the second-quantization theory.[43] To prove Eq. (14), it is enough to verify that the matrix elements of V in the basis of products of Slater determinants are the same as the matrix elements of the first-quantized operator

$$V=\sum_{i\in A}^{N_A} v_B(\mathbf{r}_i)+\sum_{j\in B}^{N_B} v_A(\mathbf{r}_j)+\sum_{i\in A}^{N_A}\sum_{j\in B}^{N_B} r_{ij}^{-1}+V_0. \quad (17)$$

One can easily check that the operators F_C, W_C, V, and H commute with the number operators $\hat{N}_A=a_\mu^\mu$ and $\hat{N}_B=b_\mu^\mu$ and, consequently, conserve the number of electrons in molecule A (or B). This means that we can limit ourselves to the (N_A+N_B)-electron Hilbert space $\mathscr{H}_A\otimes\mathscr{H}_B$ and need not consider the Fock space $\mathscr{F}_{AB}$ any further.

One should mention that the spin orbitals ϕ_μ^C do not have to be localized on the nuclei of molecule C (monomer-centered basis). When a finite basis set is used in calculations, the functions' ϕ_μ^C's must actually be localized on the nuclei of both molecules (dimer-centered basis), i.e., the linear spans of ϕ_μ^A's and ϕ_μ^B's must be identical. The use of the dimer-centered basis set is essential for calculating the exchange components of the interaction energy.

As is well known, formulas (10)–(15) are invariant under unitary transformations of spin orbitals ϕ_μ^C. Since all perturbation theory corrections considered in this article can be expressed using the the operators F_C, W_C, and V and the Hartree–Fock wave functions of the monomers, these corrections are invariant under separate unitary transformations of occupied and virtual spin orbitals. For perturbation theory development, however, it is very convenient to use the *canonical* spin orbitals which diagonalize the Fock operator f_C,

$$(f_C)_\nu^\mu=\langle\phi_\mu^C|f_C|\phi_\nu^C\rangle=\epsilon_\mu^C\delta_{\mu\nu}, \quad (18)$$

where ϵ_μ^C are the orbital energies. These orbitals will be used in all further considerations.

Since for positive energies f_C have purely continuous spectra, the virtual orbitals defined via Eq. (18) do not have well-defined limits when the number of basis set spin orbitals approaches infinity. The many-body perturbation theory can, however, be formulated in a basis set independent way[46] (this is a consequence of the unitary invariance of the theory). This formulation shows that all the corrections in Eq. (6) have well-defined limits when the basis set becomes infinitely large and complete. These limits, representing "saturated" or basis set independent values of perturbation corrections, can also be computed using variational techniques and the basis set of *explicitly* correlated Gaussian geminals.[37,46]

B. Explicitly connected polarization expansion

The Schrödinger equation for the complex AB,

$$(F+\zeta V+\xi W_A+\eta W_B)\Psi=E\Psi \quad (19)$$

can be solved using the conventional Rayleigh–Schrödinger perturbation theory in which $F=F_A+F_B$ is treated as the unperturbed operator and V, W_A, and W_B are perturbations. The corresponding zeroth-order equation is

$$F\Phi=E_0\Phi. \quad (20)$$

It is easy to see that the unperturbed wave function $\Phi=\Phi_A\Phi_B$ is the product of the HF determinants Φ_A and Φ_B for monomers A and B, and E_0 is the sum of the orbital energies of all occupied orbitals in A and B. In the conventional approach, the perturbation corrections $E_{\rm pol}^{(kij)}$ are expressed in terms of Φ, V, W_A, W_B, and the reduced resolvent of F. The expressions for $E_{\rm pol}^{(kij)}$ contain many components, which after expansion in terms of one- and two-electron integrals, contain disconnected terms (or diagrams) and, consequently, behave incorrectly when the size of the system increases. After considerable algebraic manipulations, these disconnected terms cancel out in each order of perturbation theory and the final result contains only connected terms (or diagrams), which guarantees the extensivity[3] of the energy. To avoid the above complications, we found it advantageous to formulate the perturbation theory using the coupled-cluster representation of the Schrödinger equation.[41–43,45] In this representation, the nonphysical disconnected terms do not appear at all and the perturbation energies are expressed directly in terms of connected contributions.

The coupled-cluster ansatz for the exact wave function Ψ is[29]

$$\Psi=e^T\Phi, \quad (21)$$

where

$$T=\sum_{n=0}^{N_A}\sum_{m=0}^{N_B} T_{nm}, \quad n+m>0 \quad (22)$$

is a sum of the cluster operators which create n-tuple excitations of the monomer A and m-tuple excitations of the monomer B. The explicit form of the operator T_{nm} is

$$T_{nm}=\left(\frac{1}{n!m!}\right)^2 t_{\rho_1\cdots\rho_n\sigma_1\cdots\sigma_m}^{\alpha_1\cdots\alpha_n\beta_1\cdots\beta_m} a_{\alpha_1\cdots\alpha_n}^{\rho_1\cdots\rho_n} b_{\beta_1\cdots\beta_m}^{\sigma_1\cdots\sigma_m}, \quad (23)$$

where the indices $\alpha_1\cdots\alpha_n(\rho_1\cdots\rho_n)$ label occupied (virtual) spin orbitals of the monomer A and the indices $\beta_1\cdots\beta_m(\sigma_1\cdots\sigma_m)$ label occupied (virtual) spin orbitals of the monomer B. We assume that the cluster amplitudes t are separately antisymmetric in the four groups of their indices $\alpha_1\cdots\alpha_n,\beta_1\cdots\beta_m,\rho_1\cdots\rho_n$, and $\sigma_1\cdots\sigma_m$. The t amplitudes and the T_{nm} operators are then uniquely defined by Ψ. The ansatz (21) differs from the standard exponential ansatz of the coupled-cluster theory[41,42,47,3] since $\Phi=\Phi_A\Phi_B$ is the product of two Slater determinants rather than a single determinant. Equation (21) can be derived by representing Ψ in the form of a "full configuration interaction (CI)" expansion $\Psi=(1+C)\Phi$ [with C given by equations analogous to Eqs. (22) and (23)] and by defining $T=\ln(1+C)$.

The cluster operator T and the total energy are determined from the Schrödinger equation $(H-E)\Psi=0$. Writing this equation in the form $e^{-T}(H-E)e^T\Phi=0$ and projecting against the functions

$$\Phi_{\alpha_1\cdots\alpha_n\beta_1\cdots\beta_m}^{\rho_1\cdots\rho_n\sigma_1\cdots\sigma_m}=a_{\alpha_1\cdots\alpha_n}^{\rho_1\cdots\rho_n} b_{\beta_1\cdots\beta_m}^{\sigma_1\cdots\sigma_m}\Phi$$

gives the following equation for T:

$$\langle \Phi^{\rho_1\cdots\rho_n\sigma_1\cdots\sigma_m}_{\alpha_1\cdots\alpha_n\beta_1\cdots\beta_m} | e^{-T}(F+\zeta V+\xi W_A+\eta W_B)e^{T}\Phi\rangle = 0. \tag{24}$$

Note, that the cluster operator T depends now on the expansion parameters ζ, ξ, and η, i.e., $T=T(\zeta,\xi,\eta)$. Similarly, projecting against Φ, we obtain the energy expression

$$E(\zeta,\xi,\eta) = E_0 + \langle (\zeta V+\xi W_A+\eta W_B)e^{T}\rangle, \tag{25}$$

where $\langle X\rangle$ is the "vacuum" expectation value of the operator X,

$$\langle X\rangle = \langle \Phi | X\Phi\rangle.$$

In deriving Eq. (25), we used Eq. (20) and the fact that the exact wave function Ψ satisfies here the intermediate normalization $\langle e^{T}\rangle = 1$. No approximations have been made in deriving Eqs. (24) and (25), so that for $\zeta=\xi=\eta=1$ all the exchange effects are included in $E(1,1,1)$. The exchange is neglected when a *finite-order* power series in ζ is used to approximate $E(\zeta,\xi,\eta)$ at $\zeta=1$ (Refs. 21–23). The polarization corrections $E^{(n)}_{\rm pol}$ are then defined as the coefficients in the power series expansion of $E(\zeta,1,1)$. Similarly, the intramonomer correlation corrections $E^{(nij)}_{\rm pol}$ are coefficients in the triple power series expansion of $E(\zeta,\xi,\eta)$ around $\zeta=\xi=\eta=0$.

It is easy to verify that when $\zeta=0$,

$$T(0,\xi,\eta) = T_A(\xi) + T_B(\eta) \tag{26}$$

and

$$E(0,\xi,\eta) = E_A(\xi) + E_B(\eta), \tag{27}$$

where $T_A(\xi)$ and $T_B(\eta)$ are the exact cluster operators for the molecules A and B, respectively, and $E_A(\xi)$ and $E_B(\eta)$ are the ground-state eigenvalues of the Hamiltonians $H_A+\xi W_A$ and $H_B+\eta W_B$. It follows from Eqs. (26) and (27) that $T^{(0ij)}$ and $E^{(0ij)}_{\rm pol}$ must vanish when $i>0$ and $j>0$. The corrections $E^{(0i0)}_{\rm pol}$ and $E^{(00j)}_{\rm pol}$ are just the Møller–Plesset perturbation energies for molecules A and B, respectively. All the remaining corrections $E^{(nij)}_{\rm pol}$, $n\geqslant 1$ must therefore be included in the interaction energy $E_{\rm int}$. Since $T_A(\xi)$ and $T_B(\eta)$ are the sums of the operators of the form T_{n0} and T_{0n}, respectively, Eq. (26) shows that all cluster operators T_{nm} for which $n>0$ and $m>0$ must vanish when $\zeta\to 0$, i.e., when the interaction between monomers is switched off.

The simplest way to obtain the exchange contribution in a low-order perturbation treatment is to keep Eq. (24) intact and to introduce antisymmetrization into the energy expression. The appropriate energy expression is[22,23]

$$\mathscr{E}(\zeta,\xi,\eta) = E_0 + \langle (\zeta V+\xi W_A+\eta W_B)\mathscr{A}e^{T}\rangle / \langle \mathscr{A}e^{T}\rangle, \tag{28}$$

where $T=T(\zeta,\xi,\eta)$ is defined by Eq. (24) and $\mathscr{A}$ is the full N-electron antisymmetrizer. Equation (28) is obtained when the Schrödinger equation $(H-E)e^{T}\Phi=0$ is replaced by the antisymmetrized form $(H-E)\mathscr{A}e^{T}\Phi=0$ and the scalar product of the left-hand side with Φ is set equal to zero. The cluster operator T is defined as before by Eq. (24). This method of introducing the exchange terms corresponds closely to the so-called symmetrized-polarization method of Chipman *et al.*[18] or the symmetrized Rayleigh–Schrödinger (SRS) method of Ref. 22. Other, more complicated methods of symmetry adaptation are possible[22,23] but through the second order in V they lead to results equivalent to those of the SRS method. It should be stressed that $\mathscr{E}(\zeta,\xi,\eta)$ and $E(\zeta,\xi,\eta)$ are two different analytic functions of ζ, ξ, and η, though they are equal for $\zeta=\xi=\eta=1$, i.e.,

$$\mathscr{E}(1,1,1) = E(1,1,1). \tag{29}$$

The exchange corrections to the interaction energy are defined by

$$E^{(nij)}_{\rm exch} = E^{(nij)} - E^{(nij)}_{\rm pol}, \tag{30}$$

where $E^{(nij)}$ are the coefficients in the Taylor expansion of $\mathscr{E}(\zeta,\xi,\eta)$,

$$\mathscr{E}(\zeta,\xi,\eta) = \sum_{nij} \zeta^n\xi^i\eta^j E^{(nij)}. \tag{31}$$

In the following, we shall also use double-superscript energy corrections $E^{(kl)}_{\rm pol}$ and $E^{(kl)}_{\rm exch}$ defined generally by

$$E^{(kl)} = \sum_{i=0}^{l} E^{(k,i,l-i)}.$$

They represent the intramonomer correlation effect of the lth order in the total correlation operator $W=W_A+W_B$.

To proceed further, Eq. (24) has to be transformed into a form suitable for an iterative (perturbative) solution. Using the fact that

$$e^{-T}Fe^{T} = F + [F,T],$$

it can be rewritten in the form

$$\langle a^{\rho_1\cdots\rho_n}_{\alpha_1\cdots\alpha_n} b^{\sigma_1\cdots\sigma_m}_{\beta_1\cdots\beta_m}\Phi | [F,T] + D | \Phi\rangle = 0, \tag{32}$$

where $D=e^{-T}(\zeta V+\xi W_A+\eta W_B)e^{T}$. After the commutator in Eq. (32) is expanded using, e.g., the contraction theorem,[48] one obtains

$$-\epsilon^{\alpha_1\cdots\alpha_n\beta_1\cdots\beta_m}_{\rho_1\cdots\rho_n\sigma_1\cdots\sigma_m} t^{\alpha_1\cdots\alpha_n\beta_1\cdots\beta_m}_{\rho_1\cdots\rho_n\sigma_1\cdots\sigma_m} + \langle a^{\rho_1\cdots\rho_n}_{\alpha_1\cdots\alpha_n} b^{\sigma_1\cdots\sigma_m}_{\beta_1\cdots\beta_m}\Phi | D | \Phi\rangle = 0, \tag{33}$$

where

$$\epsilon^{\alpha_1\cdots\alpha_n\beta_1\cdots\beta_m}_{\rho_1\cdots\rho_n\sigma_1\cdots\sigma_m} = \epsilon^A_{\alpha_1}+\cdots+\epsilon^A_{\alpha_n}+\epsilon^B_{\beta_1}+\cdots+\epsilon^B_{\beta_m} - \epsilon^A_{\rho_1}-\cdots-\epsilon^A_{\rho_n}-\epsilon^B_{\sigma_1}-\cdots-\epsilon^B_{\sigma_m}.$$

Note that there is no implicit summation in the formula (33) since the repeated indices are either both lower or both upper. For fixed D, Eq. (33) can be solved easily for T_{nm}. This solution can be written formally as $T_{nm}=\Re_{nm}(D)$, where $\Re_{nm}$ is the resolvent superoperator defined for an arbitrary operator X as[29]

$$\Re_{nm}(X) = \left(\frac{1}{n!m!}\right)^2 \langle a^{\alpha_1\cdots\alpha_n}_{\rho_1\cdots\rho_n} b^{\beta_1\cdots\beta_m}_{\sigma_1\cdots\sigma_m} X\rangle \times a^{\rho_1\cdots\rho_n}_{\alpha_1\cdots\alpha_n} b^{\sigma_1\cdots\sigma_m}_{\beta_1\cdots\beta_m} / \epsilon^{\alpha_1\cdots\alpha_n\beta_1\cdots\beta_m}_{\rho_1\cdots\rho_n\sigma_1\cdots\sigma_m}. \tag{34}$$

The definition (34) represents a natural generalization of the resolvent superoperator introduced in Ref. 49. Using Eq. (22) allows us to rewrite Eq. (24) in the form

$$T = \Re[e^{-T}(\zeta V+\xi W_A+\eta W_B)e^{T}], \tag{35}$$

where

$$\Re = \sum_{n=0}^{N_A}\sum_{m=0}^{N_B} \Re_{nm}, \quad n+m>0. \tag{36}$$

Equation (35) represents the main result of this section. It is ideally suited for a perturbative or an iterative solution. If an iterative procedure is initiated by assuming $T=0$ (note that for $\zeta=\xi=\eta=0$, we have $T=0$), it generates polynomials in ζ,ξ,η which after sufficiently many iterations provide the expressions for the coefficients in the series

$$T(\zeta,\xi,\eta)=\sum_{kij}\zeta^k\xi^i\eta^j T^{(kij)},\quad k+i+j>0. \tag{37}$$

Alternatively, substituting Eq. (37) into Eq. (35) and comparing coefficients at $\zeta^k\xi^i\eta^j$ gives recursive relations for $T^{(kij)}$. Inserting Eq. (37) into Eq. (25), one obtains the formulas for the individual corrections $E_{\rm pol}^{(kij)}$. In transforming Eq. (35), the following (finite) expansion is used:

$$e^{-T}Xe^{T}=X+[X,T]+\frac{1}{2!}[[X,T],T]+\cdots, \tag{38}$$

which shows that all the $T^{(kij)}$ operators and all the energy corrections $E_{\rm pol}^{(kij)}$ are expressed through commutators. Since a commutator of two second-quantized operators contains only contracted (connected) terms (diagrams), our perturbation energies and cluster operators are fully connected. Disconnected (size nonextensive) objects do not appear in the theory at all and do not have to be eliminated. This feature of our approach not only simplifies an order-by-order perturbation theory expansion, but also allows a nonperturbative treatment of intramonomer correlation effects via size-extensive infinite-order (in W_A or W_B) selective summation techniques.

In Secs. III and IV, we consider in detail the intramonomer correlation corrections through the second order in $W=W_A+W_B$ to the electrostatic and dispersion energies. We show how these corrections can be expressed in terms of the first order (in V, W_A, and W_B) cluster operators and present the final formulas in terms of molecular integrals and orbital energies. Derivation of these final formulas is discussed in the Appendices.

III. ELECTROSTATIC ENERGY

The first-order polarization energy $E_{\rm pol}^{(1)}$ represents the classical energy of the electrostatic interaction of charge distributions of unperturbed monomers. For this reason, $E_{\rm pol}^{(1)}$ is often referred to as the electrostatic energy and denoted accordingly by $E_{\rm elst}^{(1)}$. When the intramonomer correlation is neglected, $E_{\rm pol}^{(1)}$ is approximated by $E_{\rm pol}^{(10)}$, i.e., by the first term in the expansion (6). From Eq. (25), we have

$$E_{\rm pol}^{(10)}=\langle V\rangle=v_{\alpha\beta}^{\alpha\beta}+(v_A)_\beta^\beta+(v_B)_\alpha^\alpha+V_0, \tag{39}$$

which shows that $E_{\rm pol}^{(10)}$ is the energy of the electrostatic interaction of the Hartree–Fock charge distributions of the monomers.

Consider now the next two terms in the expansion (6), i.e., the corrections $E_{\rm pol}^{(110)}$ and $E_{\rm pol}^{(101)}$. From Eq. (25), we find that

$$E_{\rm pol}^{(110)}=\langle VT^{(010)}\rangle+\langle W_AT^{(100)}\rangle. \tag{40}$$

Applying Eqs. (34) and (35), we see that the first-order cluster operators $T^{(100)}$ and $T^{(010)}$ are given by

$$T^{(010)}=T_{20}^{(010)}=\Re_{20}(W_A)=\tfrac{1}{4}w_{\rho\rho'}^{\alpha\alpha'}a_{\alpha\alpha'}^{\rho\rho'}/\epsilon_{\rho\rho'}^{\alpha\alpha'} \tag{41}$$

and

$$T^{(100)}=\Re(V)=T_{10}^{(100)}+T_{01}^{(100)}+T_{11}^{(100)}, \tag{42}$$

$$T_{10}^{(100)}=\Re_{10}(V)=(\omega_B)_\rho^\alpha a_\alpha^\rho/\epsilon_\rho^\alpha, \tag{43}$$

$$T_{01}^{(100)}=\Re_{01}(V)=(\omega_A)_\sigma^\beta b_\beta^\sigma/\epsilon_\sigma^\beta, \tag{44}$$

$$T_{11}^{(100)}=\Re_{11}(V)=v_{\rho\sigma}^{\alpha\beta}a_\alpha^\rho b_\beta^\sigma/\epsilon_{\rho\sigma}^{\alpha\beta}, \tag{45}$$

where $(\omega_C)_\mu^\nu=(v_C)_\mu^\nu+v_{\mu\gamma}^{\nu\gamma}$, $\gamma\in C$ denotes a matrix element of the complete electrostatic potential ω_C of molecule C calculated using the HF density matrix

$$\omega_C(\mathbf{r})=v_C(\mathbf{r})+\sum_{\gamma\in C}\int\frac{\phi_\gamma^*(\mathbf{r}')\phi_\gamma(\mathbf{r}')}{|\mathbf{r}-\mathbf{r}'|}d\mathbf{r}'.$$

Note that the operators $T_{10}^{(010)}=\Re_{10}(W_A)$ and $T_{01}^{(001)}=\Re_{01}(W_B)$ vanish because of the Brillouin theorem so that $\Re(W_A)=\Re_{20}(W_A)$. Since the cluster operators of Eqs. (41)–(45) will appear very often in the subsequent development, we shall use the following shorthand notation: $T_A\equiv T_{20}^{(010)}$; $S_A\equiv T_{10}^{(100)}$; $S_B\equiv T_{01}^{(100)}$; $S\equiv T_{11}^{(100)}$; and $T_B\equiv T_{02}^{(001)}=\Re_{02}(W_B)$.

The first term on the right-hand side of Eq. (40) is equal to zero because V cannot annihilate a double excitation on A. The second term vanishes when the Hartree–Fock orbitals are used (Brillouin theorem). Thus $E_{\rm pol}^{(110)}$ and, consequently, $E_{\rm pol}^{(11)}$ are zero so that the leading intramonomer correlation contribution to the electrostatic energy is given by $E_{\rm pol}^{(12)}=E_{\rm pol}^{(120)}+E_{\rm pol}^{(102)}+E_{\rm pol}^{(111)}$. Let us consider the correction $E_{\rm pol}^{(120)}$ first. From Eqs. (25) and (35), we find that

$$E_{\rm pol}^{(120)}=\langle VT^{(020)}\rangle+\langle W_AT^{(110)}\rangle, \tag{46}$$

where

$$T^{(020)}=\Re([W_A,T^{(010)}]) \tag{47}$$

and

$$T^{(110)}=\Re([W_A,T^{(100)}]+[V,T^{(010)}]). \tag{48}$$

Inserting Eqs. (47) and (48) into Eq. (46), using the "Hermiticity" of the resolvent $\Re$,

$$\langle X|\Re(Y)\rangle=\langle\Re(X)|Y\rangle \tag{49}$$

and noting that only the S_A component of $T^{(100)}$ contributes, one obtains the following expression for $E_{\rm pol}^{(120)}$:

$$E_{\rm pol}^{(120)}=\langle S_A|[W_A,T_A]\rangle+\langle T_A|[W_A,S_A]\rangle+\langle T_A|[V,T_A]\rangle. \tag{50}$$

Using the Brillouin theorem, it is easy to show that the second term on the right-hand side of Eq. (50) is the complex conjugate of the first one so that $E_{\rm pol}^{(120)}$ can be written as

$$E_{\rm pol}^{(120)}=2\,{\rm Re}\langle S_A|[W_A,T_A]\rangle+\langle T_A|[V,T_A]\rangle, \tag{51}$$

where Re denotes the real part and the "inner product" $\langle X|Y\rangle$ of two operators X and Y is defined as

$$\langle X|Y\rangle\equiv\langle X\Phi|Y\Phi\rangle. \tag{52}$$

Performing integration over the coordinates of electrons of the monomer B in the second term and using Eq. (49) to eliminate S_A from the first term on the right-hand side of Eq. (51) leads to the following alternative expression for $E_{\rm pol}^{(120)}$:

$$E_{\rm pol}^{(120)}=2\,{\rm Re}\langle\Omega_B|T_{10}^{(020)}\rangle+\langle T_A|[\Omega_B,T_A]\rangle, \tag{53}$$

where $\Omega_B = (\omega_B)^{\nu}_{\mu} a^{\mu}_{\nu}$ and $T^{(020)}_{10} = \Re_{10}([W_A, T_A])$ is the leading term in the perturbation theory expansion of the one-particle cluster operator for the molecule A. It can be seen now that the first term on the right-hand side of Eq. (53) represents a contribution from single excitations, while the second term is due to double excitations on the monomer A.

Replacing A by B on the right-hand side of Eq. (51) leads to the corresponding expression for $E^{(102)}_{\rm pol}$. Using Eq. (25) and the fact that $T^{(011)}$ is zero, we see that $E^{(111)}_{\rm pol}$ is equal to $\langle W_A T^{(101)}\rangle + \langle W_B T^{(110)}\rangle$. These two terms vanish since, as one can see easily from Eq. (48), $T^{(101)}$ and $T^{(110)}$ cannot include double excitations on the monomers A and B, respectively. Thus, $E^{(111)}_{\rm pol}$ must vanish and $E^{(12)}_{\rm pol}$ is given by the sum of $E^{(120)}_{\rm pol}$ and $E^{(102)}_{\rm pol}$.

To express the matrix elements in Eqs. (51) and (53) in terms of one- and two-electron integrals, one can apply the Wick theorem[43] or the contraction theorem[45] and, subsequently, perform the necessary spin integrations. An alternative and more straightforward procedure is to represent all the operators in terms of the orbital unitary group generators[50,51] and to use the spin-free Wick theorem[52,53] to evaluate the commutators. The latter method, which is particularly useful for higher-order corrections, is described in Appendix A. It leads to the following expression for $E^{(120)}_{\rm pol}$:

$$E^{(120)}_{\rm pol} = 2\,\mathrm{Re}\,D_1 + D_2, \tag{54}$$

where

$$D_1 = \theta^{aa'}_{rr'} v^{rr'}_{ar''} t^{r''}_{a'} - \theta^{aa'}_{rr'} v^{ra''}_{aa'} t^{r'}_{a''} \tag{55}$$

and

$$D_2 = \theta^{aa'}_{rr'} (\omega_B)^{r'}_{r''} t^{rr''}_{aa'} - \theta^{aa'}_{rr'} (\omega_B)^{a''}_{a'} t^{rr'}_{aa''}. \tag{56}$$

All implicit summations in Eqs. (55) and (56) are over orbitals and are restricted by the convention that the indices $aa'\ldots$ ($rr'\ldots$) are used exclusively for the occupied (virtual) orbitals of the molecule A while the indices $bb'\ldots$ ($ss'\ldots$) are used exclusively for the occupied (virtual) orbitals of the molecule B. This convention will be used throughout this article. The symbols $t^{aa'}_{rr'}$ and t^{a}_{r} are the spin-free first-order cluster amplitudes (see Appendix A)

$$t^{aa'}_{rr'} \equiv v^{aa'}_{rr'}/\epsilon^{aa'}_{rr'}, \tag{57}$$

$$t^{a}_{r} \equiv (\omega_B)^{a}_{r}/\epsilon^{a}_{r}, \tag{58}$$

where v^{lk}_{mn} are defined by the right-hand side of Eq. (15) with the spin orbitals ϕ_μ, ϕ_ν, ϕ_λ, and ϕ_κ replaced by the orbitals ψ_m, ψ_n, ψ_l, and ψ_k, and $(\omega_B)^k_l = \langle\psi_l|\omega_B|\psi_k\rangle$ (the indices k, l, m, and n can label occupied and virtual orbitals from both molecules). For notational convenience, we use also the following definitions:

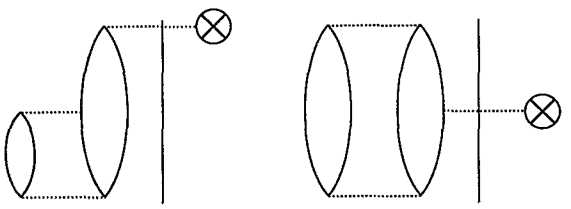

FIG. 1. Nonoriented Brandow-type diagrams representing the two terms in Eq. (54). The lines to the left (right) of the vertical line correspond to orbitals from molecule $A(B)$ (cf. Ref. 56). The crossed circle represents the Ω_B operator. The intermolecular interaction lines are not antisymmetrized.

$$\theta^{aa'}_{rr'} = 4t^{aa'}_{rr'} - 2t^{a'a}_{rr'}, \tag{59}$$

$$t^{rr'}_{aa'} \equiv (t^{aa'}_{rr'})^*, \quad t^{r}_{a} \equiv (t^{a}_{r})^*. \tag{60}$$

The two Brandow-type nonoriented diagrams[54] corresponding to expressions (55) and (56) are shown in Fig. 1. (These diagrams could also be called "partially antisymmetrized Goldstone diagrams,"[55] where *partially* signifies here that only the intramolecular interaction lines are antisymmetrized). We use the convention that the orbital lines of the molecule A (B) are drawn to the left (right) of the vertical bar[56] which "separates" the monomers. The interaction lines within the monomers correspond to antisymmetrized two-electron integrals [Eq. (12)], while the lines crossing the intermonomer border correspond to Coulomb type (nonantisymmetrized) integrals of Eq. (15). The denominator and phase rules are the same as for standard many-body perturbation theory (MBPT) diagrams. The two terms in Eqs. (55) and (56) result from assigning two possible orientations of the electron lines to each diagram.

IV. DISPERSION ENERGY

The expansion of the dispersion energy in terms of the intramonomer correlation operators W_A and W_B can be obtained in a manner similar to that described in Sec. III. The only new aspect is that the corrections of the second order in V, $E^{(2ij)}_{\rm pol}$, contain two physically distinct contributions: the dispersion component $E^{(2ij)}_{\rm disp}$ and the induction component $E^{(2ij)}_{\rm ind}$. The separation of these two components can be most easily performed by invoking the diagrammatic representation of the perturbation theory corrections. An induction energy diagram must be disconnected on one side of the intermolecular "border" since it has to contain two times the representation of the electrostatic potential of the monomer. In contrast, the dispersion energy diagrams are connected on both sides of this border. This feature is illustrated in Fig. 2. In this section, we will present a derivation and diagrammatic description of the dispersion energy corrections $E^{(2l)}_{\rm disp}$ through second order in W, i.e., for $l \leqslant 2$.

A. Hartree–Fock dispersion energy $E^{(20)}_{\rm disp}$

When the intramonomer correlation is completely neglected, the dispersion energy is approximated by the correction of the zeroth order in W_A and W_B, i.e., by $E^{(20)}_{\rm disp}$. This correction represents the dispersion interaction of molecules described at the Hartree–Fock level of approximation and therefore may be referred to as the *Hartree–Fock dispersion energy*. From Eqs. (25) and (42), we find that

$$E^{(20)}_{\rm pol} = \langle V T^{(100)}\rangle = \langle V S_A\rangle + \langle V S_B\rangle + \langle V S\rangle, \tag{61}$$

where S_A, S_B, and S were defined in the preceding section as $T^{(100)}_{10}$, $T^{(100)}_{01}$, and $T^{(100)}_{11}$, respectively. The terms $\langle V S_A\rangle$

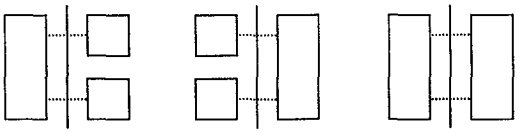

FIG. 2. General structure of induction (the first two diagrams) and dispersion energy diagrams.

and $\langle VS_B\rangle$ can be expressed through the electrostatic potential of the monomers, e.g.,

$$\langle VS_A\rangle = \langle \Omega_B|\Re_{10}(\Omega_B)\rangle = 2(\omega_B)^a_r(\omega_B)^r_a/\epsilon^a_r \quad (62)$$

and obviously constitute the induction contribution $E^{(20)}_{\rm ind}$. The dispersion part of $E^{(20)}_{\rm pol}$ is thus given by the $\langle VS\rangle$ term.

Using the spin-free forms of V and S (see Appendices A and B), one finds that

$$E^{(20)}_{\rm disp} = \langle VS\rangle = 4v^{ab}_{rs}v^{rs}_{ab}/\epsilon^{ab}_{rs}. \quad (63)$$

The above expression has a particularly simple form, so the Hartree–Fock dispersion energy can easily be calculated for large polyatomic molecules. It is worthwhile to add that $E^{(20)}_{\rm disp}$ can also be calculated variationally using arbitrary basis[29,57] by minimizing the functional $J[\tilde T_{11}] = \langle \tilde T_{11}|[F_A+F_B,\tilde T_{11}]\rangle + 2\,{\rm Re}\langle \tilde T_{11}|V\rangle$, where $\tilde T_{11}$ is a trial operator of the form of Eq. (23).

B. First-order intramonomer correlation correction $E^{(21)}_{\rm disp}$

The leading intramonomer correlation correction to $E^{(20)}_{\rm disp}$ is of the first order in W and is given by $E^{(21)}_{\rm disp}$, i.e., by the sum of $E^{(210)}_{\rm disp}$ and $E^{(201)}_{\rm disp}$. Since the appropriate expression for $E^{(201)}_{\rm disp}$ is obtained from the expression for $E^{(210)}_{\rm disp}$ by interchanging symbols pertaining to molecules A and B, below we consider only the correction $E^{(210)}_{\rm disp}$.

From Eq. (25), one can find that

$$E^{(210)}_{\rm pol} = \langle VT^{(110)}\rangle + \langle W_AT^{(200)}\rangle + \tfrac{1}{2}\langle W_A(T^{(100)})^2\rangle, \quad (64)$$

where $T^{(110)}$ is given by Eq. (48) and

$$T^{(200)} = \Re([V,T^{(100)}]). \quad (65)$$

The above expression for $T^{(200)}$ follows easily from Eqs. (35) and (38). Using Eq. (49), the first two terms on the right-hand side of Eq. (64) can be rewritten as

$$\langle V|T^{(110)}\rangle = \langle T^{(100)}|[W_A,T^{(100)}]\rangle + \langle T^{(100)}|[V,T_A]\rangle, \quad (66)$$

$$\langle W_A|T^{(200)}\rangle = \langle T_A|[V,T^{(100)}]\rangle. \quad (67)$$

Now, since we are interested in the dispersion energy, the S_A and S_B components of $T^{(100)}$ in Eqs. (66), (67), and in the third term of Eq. (64) must be neglected. These components depend on the electrostatic potential of the monomers [cf. Eqs. (43) and (44)] and contribute only to the induction energy. Thus, for our purposes, $T^{(100)}$ can be replaced by S and the dispersion part of Eq. (64) can be written as

$$E^{(210)}_{\rm disp} = \langle S|[W_A,S]\rangle + \langle S|[V,T_A]\rangle + \langle T_A|[V,S]\rangle. \quad (68)$$

Note, that the last term in Eq. (64) does not contribute since the V operator in $\langle VS^2\rangle$ cannot annihilate the quadruple excitations created by S^2. Since $\langle S|[V,T_A]\rangle = \langle [V,S]|T_A\rangle$, Eq. (68) can be rewritten in the form

$$E^{(210)}_{\rm disp} = \langle S|[W_A,S]\rangle + 2\,{\rm Re}\langle T_A|[V,S]\rangle. \quad (69)$$

The expansion of $E^{(210)}_{\rm disp}$ in terms of molecular integrals can be performed using the technique described in Appendices A and B. The result of this expansion is

$$E^{(210)}_{\rm disp} = 2t^{ab}_{rs}g^{ra'}_{ar'}t^{r's}_{a'b} + 4\,{\rm Re}\,t^{ab}_{rs}v^{a's}_{r'b}\theta^{rr'}_{aa'}, \quad (70)$$

where $\theta^{rr'}_{aa'} \equiv (\theta^{aa'}_{rr'})^*$,

$$t^{ab}_{rs} \equiv v^{ab}_{rs}/\epsilon^{ab}_{rs}, \quad t^{rs}_{ab} \equiv (t^{ab}_{rs})^* \quad (71)$$

and

$$g^{kk'}_{ll'} = 4v^{kk'}_{ll'} - 2v^{kk'}_{l'l}, \quad (72)$$

for arbitrary indices k, k', l, l' (corresponding to either occupied or unoccupied orbitals from both molecules).

The diagrams corresponding to $E^{(210)}_{\rm disp}$, i.e., to the leading (first order in W_A) correction to the Hartree–Fock dispersion energy, are of a ring type (see Fig. 3). This fact explains the success of the time-dependent HF (TDHF) or the random phase approximation (RPA) method in calculations of the van der Waals constants,[58,59] in contrast to calculations of the monomer correlation energies, where the leading correction to the second-order MBPT (MBPT2) correlation energy of a molecule contains ladder diagrams.

The correction $E^{(210)}_{\rm disp}$ and higher-order ring-type contributions to the dispersion energy are sometimes referred to as "apparent" correlation effects.[60] This terminology is a rather unfortunate extension of that used for the induction energy. Indeed, the leading (first order in W_A) correction to the "uncoupled" induction energy $E^{(200)}_{\rm ind}$ does not represent an effect of the electron correlation[28,60] since its diagrammatic representation does not involve any rings and $E^{(210)}_{\rm ind}$ is included in the HF interaction energy. However, $E^{(200)}_{\rm disp}$, $E^{(210)}_{\rm disp}$, and all the other dispersion energy corrections represent the *true* correlation since, by the very definition of the dispersion energy, their diagrammatic representation contains at least one ring (see the last diagram in Fig. 2). Clearly, no dispersion energy component is included in the HF interaction energy. Since higher $E^{(2ij)}_{\rm disp}$ corrections contain also ladders or multiple rings, we propose that $E^{(210)}_{\rm disp}$ and higher-order ring contributions are referred to as components of the *ring approximation* to the dispersion energy.

C. Second-order intramonomer correlation correction $E^{(22)}_{\rm disp}$

The intramonomer correlation correction of the second order in $W = W_A + W_B$ is given by $E^{(22)}_{\rm disp} = E^{(211)}_{\rm disp} + E^{(220)}_{\rm disp} + E^{(202)}_{\rm disp}$. Since the expression for $E^{(202)}_{\rm disp}$ can be obtained from the expression for $E^{(220)}_{\rm disp}$ by interchanging symbols pertaining to molecules A and B, it is sufficient to consider only the bilinear term $E^{(211)}_{\rm disp}$ and the term quadratic in W_A, i.e., $E^{(220)}_{\rm disp}$.

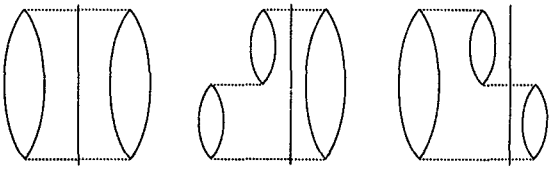

FIG. 3. Brandow-type diagrams for $E^{(200)}_{\rm disp}$ and $E^{(210)}_{\rm disp}$. The complex conjugate of the third diagram is not shown.

1. Bilinear term $E^{(211)}_{disp}$

Since the first order in W_A (W_B) intramonomer correlation correction to the electrostatic potential Ω_A (Ω_B) vanishes due to the Brillouin theorem, there is no bilinear contribution to the induction energy, i.e., $E^{(211)}_{ind} = 0$. Thus, $E^{(211)}_{pol}$ contains only a purely dispersion contribution $E^{(211)}_{pol} = E^{(211)}_{disp}$. Employing Eq. (25) and verifying that the term quadratic in T does not contribute we can write

$$E^{(211)}_{disp} = \langle W_A | T^{(201)}_{20} \rangle + \langle W_B | T^{(210)}_{02} \rangle + \langle V | T^{(111)}_{11} \rangle, \tag{73}$$

where, in view of Eq. (35),

$$T^{(201)}_{20} = \Re_{20}\{[V,T^{(101)}] + \tfrac{1}{2}[[W_B,S],S]\}, \tag{74}$$

$$T^{(210)}_{02} = \Re_{02}\{[V,T^{(110)}] + \tfrac{1}{2}[[W_A,S],S]\}, \tag{75}$$

and

$$T^{(111)}_{11} = \Re_{11}\{[W_A,T^{(101)}] + [W_B,T^{(110)}] + [[V,T_A],T_B]\}. \tag{76}$$

We only need to consider the operators $T^{(201)}_{20}$ and $T^{(210)}_{02}$ because other cluster components of $T^{(201)}$ and $T^{(210)}$ do not contribute to the matrix elements in Eq. (73). The operators $T^{(111)}_{10}$ and $T^{(111)}_{01}$ would make a contribution to the last term in Eq. (73), but they vanish due to the Brillouin theorem. Also the operators $\Re_{02}([W_A,T^{(200)}])$ and $\Re_{20}([W_B,T^{(200)}])$, which would formally contribute to $T^{(210)}_{02}$ and $T^{(201)}_{20}$, vanish because of this theorem. To illustrate the next step of the derivation, let us consider the contribution from the first term on the right-hand side of Eq. (75). Using Eq. (49) and noting that only the $T^{(110)}_{11}$ component of $T^{(110)}$ has to be considered, we can write

$$\langle T_B | [V,T^{(110)}_{11}] \rangle = \langle [V,T_B] | T^{(110)}_{11} \rangle = \langle [V,T_B] | \Re_{11}([W_A,S] + [V,T_A]) \rangle. \tag{77}$$

In the last step, we used Eq. (48) and the fact that the one-particle part of $T^{(100)}$ does not contribute. Transforming other terms in Eq. (73) in a similar way and using the (highly nontrivial) identity

$$\langle T_A | [[W_B,S],S] \rangle + \langle T_B | [[W_A,S],S] \rangle = 2\langle S | [[V,T_A],T_B] \rangle^*, \tag{78}$$

we finally find

$$E^{(211)}_{disp} = 2\,\mathrm{Re}\langle [V,T_A] + [W_A,S] | \times \Re_{11}([V,T_B] + [W_B,S]) \rangle + 2\,\mathrm{Re}\langle S | [[V,T_A],T_B] \rangle. \tag{79}$$

The Brandow-type diagrams corresponding to the above expression, given in Fig. 4, show that $E^{(211)}_{disp}$ is included in the ring approximation to the dispersion energy. The evaluation of $E^{(211)}_{disp}$ can be performed very efficiently if one proceeds in the following way: Instead of decomposing each Brandow diagram into Goldstone diagrams and computing the resulting 20 expressions diagram by diagram, one can obtain the amplitudes of $\Re_{11}([V,T_B] + [W_B,S])$ and multiply them by the amplitudes of $\Re_{11}([V,T_A] + [W_A,S])$ and by the appropriate energy denominators. The result of this procedure is

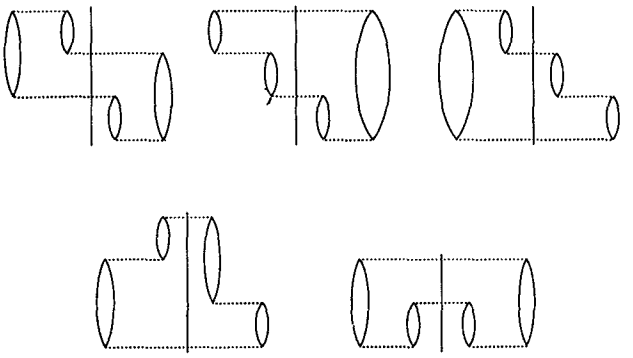

FIG. 4. Brandow-type diagrams for $E^{(211)}_{disp}$. Complex conjugate diagrams are not shown.

$$E^{(211)}_{disp} = 2P^{ab}_{rs} Q^{rs}_{ab}/\epsilon^{ab}_{rs} + 2\theta^{aa'}_{rr'}\theta^{bb'}_{ss'} v^{r's}_{a'b} t^{rs'}_{ab'}, \tag{80}$$

where P^{ab}_{rs} and $Q^{ab}_{rs} = (Q^{rs}_{ab})^*$ are proportional to the amplitudes mentioned above

$$P^{ab}_{rs} = \theta^{bb'}_{ss'} v^{as'}_{rb'} + t^{ab'}_{rs'} g^{s'b}_{b's}, \tag{81}$$

$$Q^{ab}_{rs} = \theta^{aa'}_{rr'} v^{br'}_{sa'} + t^{a'b}_{r's} g^{r'a}_{a'r}. \tag{82}$$

The quantities $\theta^{bb'}_{ss'}$ are defined in the same way as $\theta^{aa'}_{rr'}$, i.e., $\theta^{bb'}_{ss'} = 4t^{bb'}_{ss'} - 2t^{b'b}_{ss'}$, $t^{bb'}_{ss'} = v^{bb'}_{ss'}/\epsilon^{bb'}_{ss'}$ while $g^{s'b}_{b's}$ and $g^{r'a}_{a'r}$ are defined according to Eq. (72). In Eq. (80) and in all further expressions, we assume that all molecular integrals are real and we do not indicate explicitly that only the real part of an expression should be taken.

2. Quadratic term $E^{(220)}_{disp}$

In contrast to $E^{(211)}_{pol}$, the correction $E^{(220)}_{pol}$ contains both induction and dispersion contributions, which have to be separated out. According to Eq. (25), we have

$$E^{(220)}_{pol} = \langle W_A T^{(210)} \rangle + \langle V T^{(120)} \rangle + \langle W_A T^{(100)} T^{(110)} \rangle + \langle V T^{(100)} T^{(020)} \rangle. \tag{83}$$

The last two terms in the above equation depend only on the one-particle part of $T^{(100)}$ and therefore do not contribute to the dispersion energy. Also the one-particle part of $T^{(120)}$ gives purely induction contribution to $E^{(220)}_{pol}$. Generally, the dispersion part of $E^{(220)}_{pol}$ is extracted by neglecting all terms involving electrostatic potentials of the monomers. Thus, in further derivation, we only need to consider the operators $T^{(210)}_{20}$ and $T^{(120)}_{11}$. In view of Eq. (35), these operators have the following form:

$$T^{(210)}_{20} = \Re_{20}\{[W_A,T^{(200)}] + [V,T^{(110)}] + [[V,T_A],T^{(100)}]\}, \tag{84}$$

$$T^{(120)}_{11} = \Re_{11}\{[W_A,T^{(110)}] + [V,T^{(020)}] + [[W_A,T_A],T^{(100)}]\}. \tag{85}$$

Inserting Eqs. (84) and (85) into Eq. (83) and carrying out manipulations very similar to those used to derive Eq. (79), one can express the dispersion part of $E^{(220)}_{pol}$ through the first-order cluster operators T_A, T_B, and S. The resulting

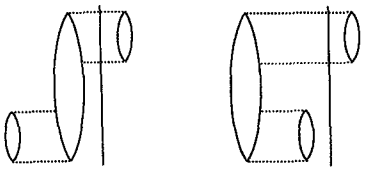

FIG. 5. Brandow-type nonoriented diagrams for $E_{\rm disp}^{(220)}(\mathrm{S})$. Two orientations are possible for each diagram. Complex conjugate diagrams are not shown.

expression for $E_{\rm pol}^{(220)}$ separates naturally into contributions, which, using the terminology commonly accepted in the many-body theory, originate from single, double, triple, and quadruple excitations

$$E_{\rm disp}^{(220)} = E_{\rm disp}^{(220)}(\mathrm{S}) + E_{\rm disp}^{(220)}(\mathrm{D}) + E_{\rm disp}^{(220)}(\mathrm{T}) + E_{\rm disp}^{(220)}(\mathrm{Q}). \tag{86}$$

The specific formulas for these contributions are

$$E_{\rm disp}^{(220)}(\mathrm{S}) = 2\,\mathrm{Re}\langle [V,S]|\Re_{10}([W_A,T_A])\rangle, \tag{87}$$

$$E_{\rm disp}^{(220)}(\mathrm{D}) = 2\,\mathrm{Re}\langle [V,S]|\Re_{20}([W_A,T_A])\rangle + \langle [V,T_A]+[W_A,S]| \times \Re_{11}([V,T_A]+[W_A,S])\rangle, \tag{88}$$

$$E_{\rm disp}^{(220)}(\mathrm{T}) = \langle [V,T_A]+[W_A,S]| \times \Re_{21}([V,T_A]+[W_A,S])\rangle, \tag{89}$$

$$E_{\rm disp}^{(220)}(\mathrm{Q}) = \langle T_A|[[V,T_A],S]\rangle + \langle S|[[W_A,T_A],S]\rangle. \tag{90}$$

It is worthwhile to note that the second term in Eq. (88) and the whole contribution from triple excitations are always negative since the resolvents $\Re_{11}$ and $\Re_{21}$ are negative definite.

All Brandow-type nonoriented diagrams representing the expressions for $E_{\rm disp}^{(220)}(\mathrm{S})$, $E_{\rm disp}^{(220)}(\mathrm{D})$, $E_{\rm disp}^{(220)}(\mathrm{T})$, and $E_{\rm disp}^{(220)}(\mathrm{Q})$ are given in Figs. 5–8. Below we present the algebraic expressions corresponding to these diagrams. The derivations of these expressions involve an extensive application of techniques described in the Appendices A and B. The

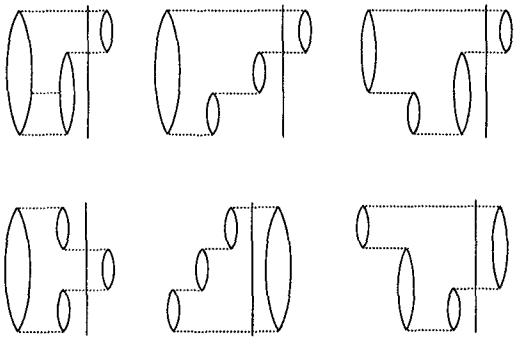

FIG. 6. Brandow-type nonoriented diagrams for $E_{\rm disp}^{(220)}(\mathrm{D})$. The first diagram has four possible orientations. Complex conjugate diagrams are not shown.

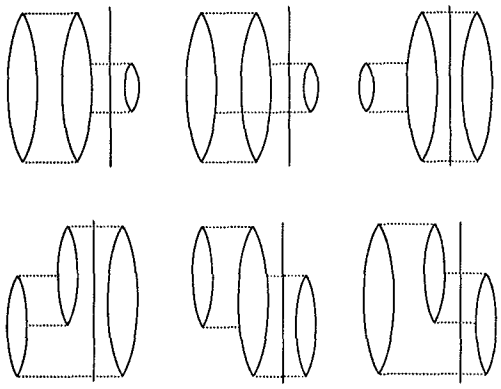

FIG. 7. Brandow-type nonoriented diagrams for $E_{\rm disp}^{(220)}(\mathrm{T})$. The first, third, and fifth diagrams have two orientations. The remaining ones have four orientations. Complex conjugate diagrams are not shown.

single, double, and triple excitations contributions to $E_{\rm disp}^{(220)}$ can be most easily obtained by evaluating the amplitudes of the operators $\Re([V,T_A])$ and $\Re([W_A,S])$ rather than by summing individual diagrams.

The corresponding formula for $E_{\rm disp}^{(220)}(\mathrm{S})$ can be written as

$$E_{\rm disp}^{(220)}(\mathrm{S}) = 4X_r^a Y_a^r/\epsilon_a^r, \tag{91}$$

where

$$X_r^a = g_{a'r'}^{r''r}\, t_{r'r''}^{aa'} - g_{a'a''}^{ar'}\, t_{rr'}^{a'a''} \tag{92}$$

and

$$Y_a^r = v_{r's}^{rb}\, t_{ab}^{r's} - v_{as}^{a'b}\, t_{a'b}^{rs}. \tag{93}$$

All symbols used above were defined previously in Eqs. (57), (71), and (72).

The formula for $E_{\rm disp}^{(220)}(\mathrm{D})$ is

$$E_{\rm disp}^{(220)}(\mathrm{D}) = (4Z_{rr'}^{aa'} - 2Z_{r'r}^{aa'})U_{aa'}^{rr'}/\epsilon_{rr'}^{aa'} + D_{ab}^{rs} D_{rs}^{ab}/\epsilon_{rs}^{ab}, \tag{94}$$

where the intermediate quantities D_{ab}^{rs}, $Z_{rr'}^{aa'}$, and $U_{aa'}^{rr'}$ are defined as follows:

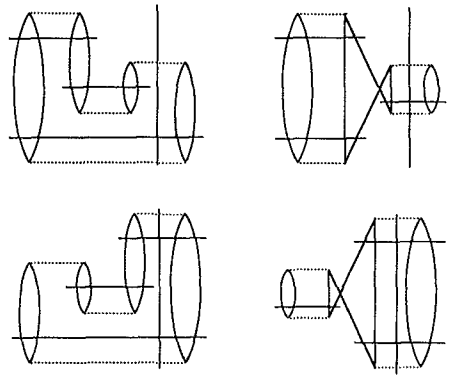

FIG. 8. Brandow-type nonoriented diagrams for $E_{\rm disp}^{(220)}(\mathrm{Q})$. The seconds and fourth diagrams have two possible orientations. Horizontal bars indicate denominators.

$$D_{rs}^{ab} = v_{a's}^{r'b}\theta_{rr'}^{aa'} + g_{ra'}^{ar'}t_{r's}^{a'b}, \tag{95}$$

$$Z_{rr'}^{aa'} = v_{rb}^{as}t_{r's}^{a'b} + v_{r'b}^{a's}t_{rs}^{ab}, \tag{96}$$

and

$$U_{aa'}^{rr'} = v_{r''r'''}^{rr'}t_{aa'}^{r''r'''} + v_{aa'}^{a''a'''}t_{a''a'''}^{rr'} + \tfrac{1}{2}v_{a'r''}^{r'a''}\theta_{aa''}^{rr''} + \tfrac{1}{2}v_{ar''}^{ra''}\theta_{a'a''}^{r'r''} - v_{a'r''}^{a''r'}t_{aa''}^{rr''} - v_{ar''}^{a''r}t_{a'a''}^{r'r''} - v_{ar''}^{a''r'}t_{a''a'}^{rr''} - v_{a'r''}^{a''r}t_{aa''}^{r''r'}. \tag{97}$$

Note that the two terms in Eq. (94) are in one to one correspondence with the two terms in Eq. (88). The Brandow-type diagrams representing these two terms are shown in Fig. 6. The first term gives a mixture of ring and ladder diagrams (shown in the first row of Fig. 6) while the second gives exclusively ring diagrams (the second row in Fig. 6).

All 48 Goldstone-type triple excitation diagrams corresponding to Brandow-type diagrams of Fig. 7 are summed using the following formula:

$$E_{\rm disp}^{(220)}(\mathrm{T}) = (4W_{rr's}^{aa'b} - 2W_{rr's}^{a'ab})W_{aa'b}^{rr's}/\epsilon_{rr's}^{aa'b}, \tag{98}$$

where

$$W_{rr's}^{aa'b} = v_{r's}^{r''b}t_{rr''}^{aa'} + v_{rs}^{r''b}t_{r''r'}^{aa'} - v_{a''s}^{a'b}t_{rr'}^{aa''} - v_{a''s}^{ab}t_{rr'}^{a''a'} + v_{rr'}^{r''a'}t_{r''s}^{ab} + v_{rr'}^{ar''}t_{r''s}^{a'b} - v_{a''r'}^{aa'}t_{rs}^{a''b} - v_{ra''}^{aa'}t_{r's}^{a''b} \tag{99}$$

and $W_{aa'b}^{rr's} = (W_{rr's}^{aa'b})^*$. The derivation of formulas (98) and (99) is given in Appendix B. Somewhat similar expression for the triple-excitation contribution to the fourth-order correlation energy of the monomer has been found by Kvasnicka.[61] It is obvious that the evaluation of the three-particle correlation contribution to the dispersion energy, given by Eqs. (98) and (99), is the most time consuming part of the evaluation of $E_{\rm disp}^{(220)}$. It should be noted that $E_{\rm disp}^{(220)}(\mathrm{T})$, similarly as $E_{\rm disp}^{(20)}$, can be calculated variationally by minimizing the functional

$$J[\tilde{T}_{21}] = \langle\tilde{T}_{21}|[F_A + F_B,\tilde{T}_{21}]\rangle + 2\,\mathrm{Re}\langle\tilde{T}_{21}|[V,T_A] + [W_A,S]\rangle, \tag{100}$$

where $\tilde{T}_{21}$ is a trial operator of the form of Eq. (23).

The quadruple excitation contribution to $E_{\rm disp}^{(220)}$ is represented by the diagrams of Fig. 8. The sum of these diagrams can be expressed as follows:

$$E_{\rm disp}^{(220)}(\mathrm{Q}) = v_{a''b}^{r''s}\theta_{aa'}^{rr'}\theta_{r'r''}^{a'a''}t_{rs}^{ab} - 2t_{aa'}^{rr''}\theta_{rr'}^{aa'}v_{a''b}^{r's}t_{r''s}^{a''b} - 2t_{aa''}^{rr'}\theta_{rr'}^{aa'}v_{a'b}^{r''s}t_{r''s}^{a''b} + t_{a''b}^{r''s}g_{aa'}^{rr'}\theta_{r'r''}^{a'a''}t_{rs}^{ab} - 2t_{rr''}^{aa'}g_{aa'}^{rr'}t_{a''b}^{r''s}t_{r's}^{a''b} - 2t_{rr''}^{aa''}g_{aa'}^{rr'}t_{a''b}^{r''s}t_{r''s}^{a'b}. \tag{101}$$

The first and the fourth terms on the right-hand side of Eq. (101) are included in the ring approximation while the remaining four, corresponding to the "cross diagrams" of Fig. 8, are not.

D. Third-order Hartree–Fock dispersion energy $E_{\rm disp}^{(30)}$

The perturbation expansion through the second order in V is expected to provide a reasonable approximation to the interaction energy in the region of the van der Waals minimum.[21–24] However, the third-order dispersion energy obtained with the complete neglect of intramonomer correlation (*the third-order Hartree–Fock dispersion energy*) is not more complicated than the terms considered thus far and can be easily included in our expansion. The magnitude of this correction will give us an indication as to the rate of convergence of the perturbation expansion for many-electron systems. Using Eqs. (25), (65), and (49), one can easily show that the third-order polarization energy $E_{\rm pol}^{(30)}$ can be written as

$$E_{\rm pol}^{(30)} = \langle T^{(100)}|[V,T^{(100)}]\rangle + \tfrac{1}{2}\langle V(T^{(100)})^2\rangle. \tag{102}$$

Since the one-particle components of $T^{(100)}$ depend on the electrostatic field of the monomers, it is obvious that only the $\langle S|[V,S]\rangle$ part of the first matrix element in Eq. (102) can contain the dispersion contribution. It turns out that after expansion in terms of molecular integrals, $\langle S|[V,S]\rangle$ contains both the pure dispersion and the induction-dispersion diagrams. The latter involve one vertex of the electrostatic potential ω_C and are *disconnected* on one side of the intermolecular border. Keeping only the pure dispersion terms, one obtains

$$E_{\rm disp}^{(30)} = 4(t_{rs}^{a'b'}v_{a'b'}^{ab}t_{ab}^{rs} - t_{rs}^{ab}v_{r'b}^{rb'}t_{ab'}^{r's} - t_{rs}^{ab}v_{as'}^{a's}t_{a'b}^{rs'} + t_{rs}^{ab}v_{r's'}^{rs}t_{ab}^{r's'}). \tag{103}$$

The Brandow-type nonoriented diagram representing the right-hand side of Eq. (103) is given in Fig. 9. The first term on the right-hand side of Eq. (103) corresponds to the hole–hole diagram variant of the nonoriented diagram, the second and third terms correspond to the particle–hole diagram, and the fourth term corresponds to the particle–particle diagram.

V. EXCHANGE CORRECTIONS

In this section, we will give expressions for the leading exchange corrections of SAPT $E_{\rm exch}^{(10)}$ and $E_{\rm exch\text{-}disp}^{(20)}$. Another significant exchange correction is $E_{\rm exch\text{-}ind}^{(20)}$. This correction, however, is already included in the SCF interaction energy. The complete expression for $E_{\rm exch}^{(10)}$ was given in Ref. 38. In deriving expressions for the exchange corrections, one usually applies the so-called S^2 or *single-exchange* approximation, i.e., retains only the terms bilinear in the orbital overlap

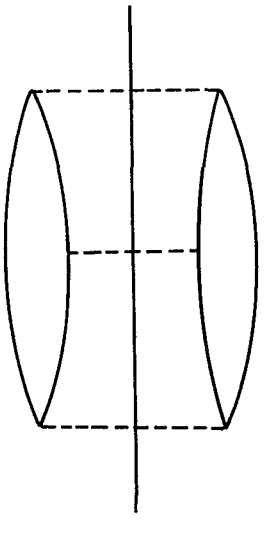

FIG. 9. Brandow-type nonoriented diagram for $E_{\rm disp}^{(300)}$ energy. This diagram has four possible orientations.

densities $\rho_{ij}^{AB}(\mathbf{r}) = \psi_i^A(\mathbf{r})\psi_j^B(\mathbf{r})$, where ψ_i^A and ψ_j^B are the orbitals of monomers A and B, respectively. With this approximation, the leading, single-exchange term in the first-order exchange energy can be written as

$$E_{\text{exch}}^{(10)} = \langle VP\rangle - \langle V\rangle\langle P\rangle, \tag{104}$$

where

$$P = -\sum_{i\in A}\sum_{j\in B} P_{ij}$$

is the sum of all single exchanges P_{ij} of electrons between systems A and B. The explicit expression for $E_{\text{exch}}^{(10)}$ in the S^2 approximation is

$$\begin{aligned} E_{\text{exch}}^{(10)} = & -2\big[\tilde{v}_{ab}^{ba} + S_{a'}^{b}(2\tilde{v}_{ab}^{aa'} - \tilde{v}_{ab}^{a'a}) \\ & + S_{b'}^{a}(2\tilde{v}_{ab}^{b'b} - \tilde{v}_{ab}^{bb'}) - 2S_{a'}^{b}S_{b'}^{a}\tilde{v}_{ab}^{ab'} \\ & - 2S_{a'}^{b'}S_{b'}^{a}\tilde{v}_{ab}^{a'b} + S_{a'}^{b}S_{b'}^{a}\tilde{v}_{ab}^{a'b'}\big], \end{aligned} \tag{105}$$

where

$$\begin{aligned} \tilde{v}_{ij}^{kl} = & v_{ij}^{kl} + (v_A)_j^l\delta_i^k/N_A + (v_B)_i^k\delta_j^l/N_B \\ & + \delta_i^k\delta_j^l V_0/(N_A N_B) \end{aligned} \tag{106}$$

and $S_b^a = \langle\psi_b^B|\psi_a^A\rangle$ is the orbital overlap integral. Notice that we use the letter S to also denote the $T_{11}^{(100)}$ operator; the meaning of this symbol will be, however, always obvious from the context.

An expression for the second-order exchange-dispersion energy in the S^2 approximations was presented in Ref. 39. This expression corresponds to the simplest possible symmetry adaptation, i.e., to the SRS expansion[22] or to the so-called Murrell–Shaw–Musher–Amos (MSMA)[19,20] method. The expression given in Ref. 39 was written in terms of geminals. Below we present an orbital version, which is more suitable for computational implementations. The $E_{\text{exch-disp}}^{(20)}$ correction in the S^2 approximation can be written as

$$E_{\text{exch-disp}}^{(20)} = \langle (V - \langle V\rangle)(P - \langle P\rangle)S\rangle. \tag{107}$$

In terms of one- and two-electron orbital integrals, this correction can be expressed as

$$E_{\text{exch-disp}}^{(20)} = -2(\tilde{v}_{ab}^{sr} + h_{ab}^{rs} + q_{ab}^{rs})t_{rs}^{ab}, \tag{108}$$

where the quantities h_{ab}^{rs} and q_{ab}^{rs} contain the hybrid and the Coulomb integrals, respectively, and are defined by

$$\begin{aligned} h_{ab}^{rs} = & S_a^s(2\tilde{v}_{a'b}^{a'r} - \tilde{v}_{a'b}^{ra'}) + S_{a'}^{s}(2\tilde{v}_{ab}^{ra'} - \tilde{v}_{ab}^{a'r}) \\ & + S_b^r(2\tilde{v}_{ab'}^{sb'} - \tilde{v}_{ab'}^{b's}) + S_{b'}^{r}(2\tilde{v}_{ab}^{b's} - \tilde{v}_{ab}^{sb'}), \end{aligned} \tag{109}$$

$$\begin{aligned} q_{ab}^{rs} = & S_b^r S_{a'}^{b'}\tilde{v}_{ab'}^{a's} - 2S_{b'}^{r}S_{a'}^{b'}\tilde{v}_{a'b}^{a's} - 2S_b^r S_a^{b'}\tilde{v}_{a'b'}^{a's} \\ & + 4S_{b'}^{r}S_a^{b'}\tilde{v}_{a'b}^{a's} + S_a^s S_b^{a'}\tilde{v}_{a'b'}^{rb'} - 2S_{a'}^{s}S_b^{a'}\tilde{v}_{ab'}^{rb'} \\ & - 2S_a^s S_{b'}^{a'}\tilde{v}_{a'b}^{rb'} + 4S_{a'}^{s}S_{b'}^{a'}\tilde{v}_{ab}^{rb'} + S_{b'}^{r}S_{a'}^{s}\tilde{v}_{ab}^{a'b'} \\ & - 2S_b^r S_{a'}^{s}\tilde{v}_{ab'}^{a'b'} - 2S_{b'}^{r}S_a^s\tilde{v}_{a'b}^{a'b'} + S_b^{a'}S_a^{b'}\tilde{v}_{a'b'}^{rs} \\ & - 2S_b^{a'}S_{a'}^{b'}\tilde{v}_{ab'}^{rs} - 2S_{b'}^{a'}S_a^{b'}\tilde{v}_{a'b}^{rs}. \end{aligned} \tag{110}$$

We would like to correct here some misprints in the formula of Ref. 39. The operators in the first three matrix elements of Eq. (25) should be v_{21}, $(1+P_{23})v_{32}$, and $(1+P_{13})v_{13}$, respectively; the first line of Eq. (26) should read

$$\begin{aligned} & 2\langle u_{ij}a_k|v_{13}(1-2P_{12})a_k a_i b_j\rangle \\ & \quad + 2\langle u_{ij}a_k|v_{31}(1-2P_{23})b_j a_k a_i\rangle \end{aligned}$$

and in the first matrix element of Eq. (27), v_{12} should be replaced by v_{32}.

VI. NUMERICAL RESULTS AND DISCUSSION

In this section, we describe numerical calculations for two medium size systems—the water dimer and the hydrogen fluoride dimer. These calculations illustrate the performance of the theory developed in the preceding sections and at the same time provide benchmark results for the investigated systems. We have used in the calculations a variety of basis sets including sets with up to f-type orbitals. Besides the many-body SAPT corrections, we have also computed the SCF and MBPT supermolecular interaction energies. The SCF and MBPT computations have been performed using the Gaussian86 package.[62]

A. Basis sets and geometries

In order to fully account for the penetration effects, all the interaction energy components were calculated with the dimer basis set. Our basis sets were constructed using the guidelines from Ref. 10. It was shown there that double-zeta quality isotropic parts are sufficient at the levels of accuracy we are interested in. Thus, isotropic parts of our bases were mainly represented by the Dunning's $[4s2p/2s]$ contractions[63] of Huzinaga's[64] $(9s5p/4s)$ GTO sets (with a 1.2 scale factor for hydrogen). This type of basis is denoted by the symbol D. To examine how the increase of the isotropic part would influence our corrections, we have performed some calculations using near triple-zeta quality bases. The first one, denoted by T^-, represents a simple extension of Dunning's double-zeta set. We have augmented this basis by adding diffuse s and p exponents equal to 0.0862 and 0.0636, respectively, on the O atom and a diffuse s exponent equal to 0.0335 on the H atom. The numerical values of these exponents have been obtained by assuming that the two smallest exponents in the original set are a part of an even tempered set and by computing the exponent which would have preceded them. This addition has been motivated by the observation made in Ref. 10 that basis sets with relatively large polarization exponents behave well if they are supplemented with diffuse s functions. The second near triple-zeta quality basis, denoted by T^{-s}, was taken from the work of Sadlej.[65] This set contains $[4s2p/2s]$ contractions of van Duijneveldt's[66] $(9s5p/4s)$ GTOs plus diffuse functions according to an analogous procedure as described above (but not identical to those in T^-). We use the symbol "-" to show that these bases are slightly smaller than a regular triple-zeta one.

These isotropic functions were combined with several sets of polarization functions. The exponents used in the polarization functions are listed in Table II. It has been shown in Ref. 10 [as well as in other papers (see Ref. 10 for references)] that standard (large) polarization exponents opti-

TABLE II. Values of the polarization functions exponents. For the basis sets from Ref. 65, the exponents are followed (in parentheses) by the contraction coefficients.

Polarization functions	Water				References
	ζ_d^O	ζ_p^H	ζ_f^O	ζ_d^H	
$(d,p)'$	0.25	0.15			67
$(d,p)^*$	0.35	0.29			10
$(2d,2p)^*$	1.007 0.292	0.392 0.142			10
$(2d,2p)^\dagger$	2.3062(0.202 70) + 0.7232(0.5791)	1.1588(0.188 44) + 0.3258(0.882 42)			
	0.2149(0.785 45) + 0.0639(0.533 87)	0.1027(0.117 80) + 0.0324(0.004 20)			65
$(2df,2pd)^*$	1.007 0.292	0.392 0.142	0.319	0.403	10
	Hydrogen fluoride				
	ζ_d^F	ζ_p^H	ζ_f^F	ζ_d^H	
$(d,p)'$	0.25	0.15			67
$(2d,2p)'$	1.0 0.15	1.0 0.08			67
$(2d,2p)^\dagger$	2.9532(0.183 54) + 0.9186(0.510 58)	1.1588(0.188 44) + 0.3258(0.882 42)			
	0.2668(0.699 25) + 0.0775(0.429 26)	0.1027(0.117 80) + 0.0324(0.004 20)			65
$(2df,2dp)^\dagger$	The same as above	The same as above	0.275	0.075	65, 70

mized for monomer's correlation energies should not be used for interaction energy calculations. Therefore, in this study we have used only diffuse polarization functions. The polarization exponents for water and hydrogen fluoride, denoted by $(d,p)'$, were determined by van Duijneveldt and van Duijneveldt–van de Rijdt (vDvD)[67] (see also Ref. 68) and they represent a compromise between even smaller values needed for getting reliable polarizabilities and larger ones required for electric multipole moments. The $(d,p)^*$, $(2d,2p)^*$, and $(2df,2pd)^*$ exponents for water were determined in Ref. 10 by optimizing the dispersion interaction between two water molecules. The $(2d,2p)^\dagger$ exponents were obtained by Sadlej[65] within the basis set polarization approach[69] to optimize atomic Hartree–Fock polarizabilities. The $(2df,2pd)^\dagger$ set for HF contains in addition the second polarization shell taken from the work of Diercksen and Sadlej.[70] The $(2d,2p)'$ exponents for hydrogen fluoride were used by vDvD in their doubly polarized basis sets and are close to the values that maximize the dipole polarizability of HF. We have always used five component d and seven component f orbitals, unless noted otherwise.

We have used two slightly different monomer geometries for water. The first one has been exactly the same as the one adopted in Refs. 10 and 57. It has been applied for a single-point calculation in a near-equilibrium dimer's geometry. The second monomer's geometry, which was used for all other calculations, was taken from Ref. 71. The two geometries have virtually the same bond length and differ by only 0.4° in the HOH angle.

Our most extensive calculations for $(H_2O)_2$ have been performed in the same near-equilibrium dimer's configuration as used in Refs. 10 and 57. In this configuration, the proton donor (molecule A) is in the xy plane with the oxygen atom and one hydrogen atom on the x axis. The proton acceptor (molecule B) has its oxygen on the x axis as well, the O–O distance being 5.67 bohr (3.00 Å) and the xy plane is the symmetry plane for this molecule. The angle between the O–O axis and the HOH bisector of the proton acceptor is 150° (we will denote this angle by β). The values of the nuclear coordinates for this configuration of the dimer and with the former of two monomers' geometries discussed above can be found in Ref. 10. Analogous values with the latter of a monomer's geometries are given in Table III.

To determine the minimum dimer geometry for water, we proceeded as follows: We fixed molecule A and the position of oxygen of molecule B such that the distance between O–O was 5.67 bohr, the distance close to the hydrogen bond minimum for water. We then performed calculations using both SAPT and MBPT4 methods for $\beta = 120°$, 150°, and 180°. Next, for the minimum angle, we have computed the intermolecular potential energy curves varying the O–O distance.

Our calculations for the HF dimer were less thorough since we performed them mainly to check if our conclusions about the performance of many-body SAPT based on the water dimer case will hold for other molecules as well. Thus, these calculations were done for only three geometries of this complex. The first two geometries are for the linear configu-

TABLE III. Nuclear coordinates for the near-equilibrium geometry of the water dimer (in bohrs). The monomer's geometry is from Ref. 71, the dimer's configuration is the same as used in Ref. 10 (see the text). The OH distance is 1.808 85 bohr, the HOH angle is 104.52°, and the angle between the O–O axis and the HOH bisector of the proton acceptor is 150°.

Atom	x	y	z
O	0.0	0.0	0.0
H	1.808 85	0.0	0.0
H	−0.453 63	1.751 04	0.0
O	5.669 18	0.0	0.0
H	6.627 96	−0.553 55	1.430 47
H	6.627 96	−0.553 55	−1.430 47

TABLE IV. Nuclear coordinates for the equilibrium geometry of the hydrogen fluoride dimer (in bohrs). The H–F bond length is 1.7215 bohr, the angle between the proton donor and the F···F line is equal to 5.5°, while the proton acceptor makes an angle of 68° with this line.

Atom	x	y	z
F	0.0	0.0	0.0
H	1.713 62	0.165 00	0.0
F	5.213 76	0.0	0.0
H	5.858 66	−1.596 18	0.0

ration: attractive F–H···F–H with H···F (hydrogen bond) distance of 3.56 bohr and strongly repulsive F–H···H–F with H···H distance equal to 2 bohrs. For both geometries, we have assumed the H–F bond length equals 1.7328 bohr. To compare with the literature theoretical work, we have included a third geometry which is nonlinear. The coordinates were taken from the work of Frisch *et al.*[72] This geometry has been obtained from second-order MBPT calculations with a 6-311 + + G(2*d*,2*p*) basis set and it is in good agreement with the experimental structure of $(HF)_2$ determined by Howard, Dyke, and Klemperer.[73] The Cartesian coordinates for this geometry are shown in Table IV. The HF bond length for this geometry is 1.7215 bohr. The HF molecules are in the *xy* plane with molecule *A* (proton donor) nearly along the *x* axis, while the proton acceptor makes an angle of 68° with this axis. The hydrogen bond distance is 3.50 bohr, similar to the attractive linear configuration.

B. SAPT corrections for near-equilibrium geometry of the water dimer

To investigate the dependence of the interaction energy corrections on the size of the basis set and to compare them with the components computed using the supermolecular approach, we have performed extensive single-point calculations in the geometry of Refs. 10 and 57. In Table V and in

TABLE V. SCF, many-body SAPT, and supermolecular MBPT interaction energy components for $(H_2O)_2$ in the near equilibrium geometry from Ref. 10. All energies are in kcal/mol (1 hartree = 627.51 kcal/mol). For the supermolecular approach, the subscript CP(NCP) means that the CP correction was (not) included in the calculation. For the total interaction energies, the SCF component was always taken with the CP correction included. The symbol MBPT*n* denotes the supermolecular MBPT approach through *n*th order.

Component	$D(d,p)'$	$D(d,p)^*$	$D^+(2d,p)^*$	$D(2d,2p)^*$	$T^-(2d,2p)^*$	$T^{-S}(2d,2p)^\dagger$	$D(2df,2pd)^*$
ΔE^{SCF}_{NCP}	−4.85	−5.00	−4.03	−4.10	−4.06	−4.15	−4.30
ΔE^{SCF}_{CP}	−4.04	−4.00	−3.87	−3.60	−3.70	−3.65	−3.62
$E^{(10)}_{pol}$	−7.12	−6.99	−6.92	−6.64	−6.70	−6.63	−6.64
$E^{(10)}_{exch}$	4.57	4.51	4.52	4.57	4.54	4.51	4.56
$E^{(12)}_{pol}$	0.47	0.38	0.21	0.38	0.38	0.38	0.40
$E^{(20)}_{ind}$	−1.58	−1.59	−1.56	−1.58	−1.59	−1.58	−1.58
$E^{(20)}_{disp}$	−1.35	−1.57	−1.53	−1.74	−1.75	−1.70	−1.90
$E^{(20)}_{exch\text{-}disp}$	0.21	0.25	0.25	0.27	0.27	0.27	0.30
$E^{(21)}_{disp}$	0.02	0.03	0.08	0.05	0.05	0.06	0.04
$E^{(22)}_{disp}$	−0.33	−0.35	−0.26	−0.36	−0.38	−0.37	−0.41
$E^{(30)}_{disp}$	0.00	0.02	0.02	0.03	0.03	0.03	0.06
$\Delta E^{(2)}_{NCP}$	−2.38	−1.92	−1.61	−1.93	−2.06	−2.43	−2.37
$\Delta E^{(2)}_{CP}$	−0.17	−0.47	−0.66	−0.62	−0.67	−0.62	−0.74
$\Delta E^{(3)}_{NCP}$	0.06	0.12	0.17	0.15	0.09	0.10	0.19
$\Delta E^{(3)}_{CP}$	−0.03	0.02	0.15	0.02	0.02	0.04	−0.01
$\Delta E^{(4)}_{NCP}$(SDQ)	0.02	0.01	0.07	0.08	0.12	0.13	0.10
$\Delta E^{(4)}_{CP}$(SDQ)	0.13	0.09	0.11	0.13	0.12	0.12	0.13
$\Delta E^{(4)}_{NCP}$(SDTQ)	−0.22	−0.21	−0.09	−0.17	−0.12	−0.19	−0.17
$\Delta E^{(4)}_{CP}$(SDTQ)	0.04	−0.02	−0.02	0.02	0.00	0.01	0.01
$E^{(12)}_{pol} + E^{(20)}_{disp} + E^{(20)}_{exch\text{-}disp}$	−0.67	−0.94	−1.07	−1.09	−1.10	−1.05	−1.20
δ[b]	0.50	0.47	0.41	0.47	0.43	0.43	0.46
$E^{(10)} + E^{(20)}_{ind}$	−4.13	−4.07	−3.96	−3.65	−3.75	−3.70	−3.66
$SAPT_{corr}$[c]	−0.98	−1.24	−1.23	−1.37	−1.40	−1.33	−1.51
SAPT	−5.11	−5.31	−5.19	−5.02	−5.15	−5.03	−5.17
SCF + $SAPT_{corr}$[d]	−5.02	−5.24	−5.10	−4.97	−5.10	−4.98	−5.13
$MBPT4_{CP}$	−0.16	−0.47	−0.53	−0.58	−0.65	−0.57	−0.74
SCF + $MBPT2_{NCP}$	−6.42	−5.92	−5.48	−5.53	−5.76	−6.08	−5.99
SCF + $MBPT2_{CP}$	−4.21	−4.47	−4.53	−4.22	−4.37	−4.27	−4.36
SCF + $MBPT4_{NCP}$	−6.58	−6.05	−5.40	−5.55	−5.79	−6.18	−5.97
SCF + $MBPT4_{CP}$	−4.20	−4.47	−4.40	−4.18	−4.35	−4.22	−4.36

[a] Basis set from Ref. 57 with six-component *d* orbitals.
[b] $\delta = \Delta E^{(2)}_{CP} - (E^{(12)}_{pol} + E^{(20)}_{disp} + E^{(20)}_{exch\text{-}disp})$.
[c] The sum of all SAPT corrections except for $E^{(10)}$ and $E^{(20)}_{ind}$.
[d] $\Delta E^{SCF}_{CP} + SAPT_{corr}$.

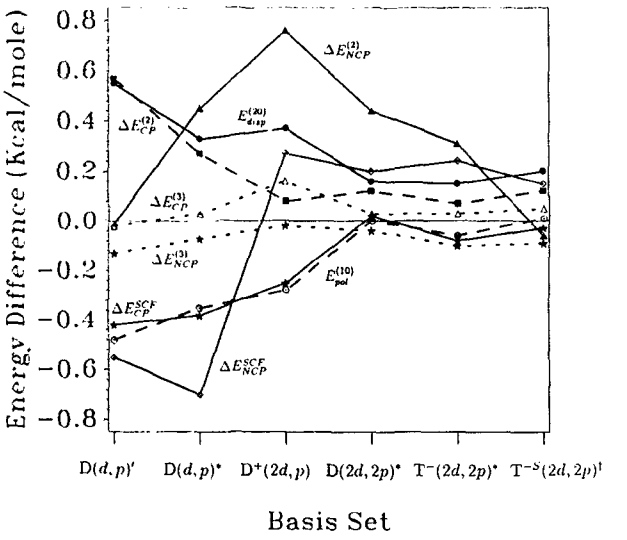

FIG. 10. The energy difference between the result in our largest basis set and those in the smaller basis sets. The curves are shown only for those components which differ by more than 0.1 kcal/mol for at least one basis set. The points on the horizontal axis are the consecutive basis sets from Table V. The curves are: diamonds—ΔE^{SCF}_{NCP}; open stars—ΔE^{SCF}_{CP}; open circles—$E^{(10)}_{pol}$; triangles—$\Delta E^{(2)}_{NCP}$; squares—$\Delta E^{(2)}_{CP}$; full stars—$\Delta E^{(3)}_{NCP}$; open triangles—$\Delta E^{(3)}_{CP}$; dots—$E^{(20)}_{disp}$. The lines joining the marks are drawn only to guide the eye.

Fig. 10, we present the many-body SAPT energy components as well as SCF and MBPT supermolecular interaction energies obtained using basis sets ranging in size from 50 to 106 terms. (These basis sets, despite similarities, are all distinct from those used in Ref. 10). All SAPT corrections were calculated from the expressions given in Secs. III–V except for the exchange correction $E^{(10)}_{exch}$ which was computed from the complete formula (valid through all orders of the overlap densities ρ^{AB}_{ij}) given in Ref. 38. We have also included total interaction energies obtained by summing proper components. Since it has been shown recently that at the SCF level the counterpoise (CP) correction should always be applied (see the discussion and literature references in Ref. 10), we will use only the CP corrected SCF energies in our further considerations. Thus, if a summed quantity contains the SCF interaction energy, this energy is always computed with the CP correction. The CP uncorrected SCF interaction energies (denoted by NCP) are, however, listed in Table V. The limit value of the SCF interaction energy for $(H_2O)_2$ at the discussed geometry is probably very close to -3.73 kcal/mol, i.e., to the energy computed in Ref. 10 in a very large 212-term basis set. The present value of the SCF interaction energy (with the CP correction) in our largest $D(2df,2pd)$* basis is quite close (within 0.1 kcal/mol) to the limit value. The SAPT interaction energy displayed in Table V is the sum of all the many-body SAPT corrections computed by us. The SCF + $SAPT_{corr}$ energy is obtained by adding to the SCF interaction energy all those corrections except for $E^{(10)}$ and $E^{(20)}_{ind}$. The SCF + MBPTn energies include the sums of the supermolecular MBPT corrections through nth order.

The atomic basis set $D^+(2d,p)$ in Table V is identical to that used in Ref. 57. Our values of the corrections $E^{(10)}$, $E^{(20)}_{ind}$, and $E^{(20)}_{disp}$ are, however, slightly different from those computed in Ref. 57. This difference results from the fact that in Ref. 57 the occupied orbitals were expanded using only the monomer basis set, while in our work the full dimer basis set was used. The MBPT corrections in this basis set have been computed previously by Harrison and Bartlett.[74] Small differences between our energies and those of Ref. 74 result from the frozen-core approximation employed in the latter work.

After this paper had been submitted, we became aware of the recently published work by Hess *et al.*[75] These authors computed the $E^{(10)}_{pol}$, $E^{(10)}_{exch}$, $E^{(20)}_{ind}$, $E^{(20)}_{exch\text{-}ind}$, $E^{(20)}_{disp}$, and $E^{(20)}_{exch\text{-}disp}$ corrections for the water dimer. Although one of their geometries and one of their basis sets is identical to those included by us, their numerical results are somewhat different than the respective results obtained in this paper. For example, their $E^{(20)}_{exch\text{-}disp}$ at $R = 5.67$ is 0.27 kcal/mol, while we obtained 0.25 kcal/mol. The difference is due to the fact that, while we consistently use a dimer-centered basis set, in the work of Hess *et al.*, similarly as in Ref. 57, the occupied orbitals and the Fock operators for the monomers are constructed using monomer-centered basis sets and only the virtual orbitals are expanded in a dimer-centered basis set (these virtual orbitals diagonalize the Fock operators obtained previously with a monomer-centered basis set).

Despite the wide range of the basis sets explored, the many-body SAPT corrections presented in Table V show a remarkable stability. Already the smallest bases give realistic values of all the corrections. The total SAPT interaction energies are all within 0.15 kcal/mol of the largest basis set result. The slowest convergence with the basis set is obtained for the $E^{(20)}_{disp}$ correction. This is probably due to the fact that higher angular functions are necessary to correctly represent the long-range multipolar part of $E^{(20)}_{disp}$ and to the upper-bounding property of the functional determining this correction. The other relatively slowly convergent correction is $E^{(10)}_{pol}$, which is connected with the somewhat slow basis set convergence of the multipole moments for the water molecule. Since these two corrections are among the least time consuming ones, large basis sets can be applied to compute their values accurately. Table V also shows that the exchange corrections $E^{(10)}_{exch}$ and $E^{(20)}_{exch\text{-}disp}$ exhibit even lesser dependence on the size of the basis set than the polarization ones. This observation shows that in the dimer-centered basis sets, the wave function converges faster in the region of space between the two molecules (which gives major contributions to the exchange components) than in the other regions. One should recall here that the exchange corrections are very slowly convergent in monomer-centered basis sets.[1,2,57,76–78] The convergence patterns shown in Table V allow us to roughly estimate that the error of particular SAPT corrections computed with our largest $D(2df,2pd)$* basis is not larger than 0.1 kcal/mol.

With the time of calculations strongly dependent on the number of basis functions, it is very important to use optimal basis sets. Results of Table V show (see also Ref. 10) that among the possible improvements over the 50-term $D(d,p)'$ basis, the most important is the addition of the second set of

(d,p)-type polarization functions (which increases the size of the basis set by 22 orbitals). This addition changes significantly both the first-order energy and the dispersion energy. Augmenting the isotropic part of the basis set to the T^- quality has a smaller effect than adding a set of (f,d)-type polarization functions, however, the former change increases the basis set by 12 terms only while the latter increases it by 34 terms. The extension of the isotropic part changes practically only the first-order components. Since the SCF CP-corrected energy in the $T^-(2d,2p)^*$ basis set is very close to the limit value,[10] a further increase of the isotropic part of the basis set would be irrelevant.

Since it would be impractical with the computer resources available to us to compute the potential energy surface for the water dimer in the largest basis set presented in Table V, these calculations have been performed in a smaller $T^-(2d,2p)$-type basis. Of two such sets (of identical size) included in Table V, the set $T^-(2d,2p)^*$ provides somewhat better energies, both at the SCF and the dispersion energy levels and therefore this set has been used in all other calculations for the water dimer. The diffuse s and p functions included in this set remedy a difficulty connected with the use of the dispersion-energy-optimized polarization exponents. Such exponents are larger than those recommended by vDvD[67] and therefore they are somewhat less effective than the latter ones in describing the polarization and multipole interaction effects. The closeness of the SCF energy computed with the $T^-(2d,2p)^*$ basis to the limit value demonstrates that these effects are now reproduced very accurately.

A more detailed breakup of $E_{\rm disp}^{(2)}$ into various components is given in Table VI. The convergence of the many-body expansion of $E_{\rm disp}^{(2)}$ is not particularly fast. The $E_{\rm disp}^{(22)}$ component is equal to about one fifth of the $E_{\rm disp}^{(20)}$ energy. It should be noted that the very small value of the $E_{\rm disp}^{(21)}$ correction results from a cancellation of the relatively large contributions from the second and third diagrams in Fig. 3. Thus, the smallness of $E_{\rm disp}^{(21)}$ is probably accidental for ten-electron systems. This correction actually plays an important role for the helium dimer.[29,37] Similar cancellations are not observed for the $E_{\rm disp}^{(211)}$ correction. This correction is negligible due to small contributions from both double and quadruple excitation diagrams. In the case of the $E_{\rm disp}^{(22)}$ correction, the largest contributions are given by the single and triple excitation diagrams. The contribution from the quadruple excitation diagrams is positive and diminishes the overall $E_{\rm disp}^{(22)}$ correction by about 30%. The contribution from the double excitation diagrams is negligible due to a cancellation of ring and ring–ladder diagrams (shown in Fig. 6).

The stability with the basis set of our SAPT energies contrasts with a rather erratic behavior of the supermolecular corrections shown in Table V (for more examples at the same geometry, see Table V of Ref. 10). In addition, the supermolecular results computed with and without the CP correction differ dramatically. In the CP-uncorrected approach, both the individual corrections and their sum show undulatory character and a very slow convergence with the basis set. If the CP-uncorrected values are discarded, however, the convergence of the supermolecular method appears to be uniform and faster. Moreover, the convergence pattern can now be rationalized by comparison with the many-body SAPT corrections. From Fig. 10, it is seen that the convergence of $\Delta E_{\rm CP}^{\rm SCF}$ is clearly determined by the convergence of $E_{\rm pol}^{(10)}$. The remaining SAPT corrections contributing to $\Delta E_{\rm CP}^{\rm SCF}$ (see discussion below) converge very rapidly. Next, the convergence of $\Delta E_{\rm CP}^{(2)}$ follows closely that of $E_{\rm disp}^{(20)}$. The $\Delta E_{\rm CP}^{(3)}$ and $\Delta E_{\rm CP}^{(4)}$(SDTQ) corrections seem to behave somewhat erratically; this fact, however, is clearly due to their very small values. Since these corrections are so small, the total supermolecular interaction energy is determined practically by the SCF and the second-order terms. The consistency of the convergence patterns of the CP-corrected supermolecular energies with the many-body SAPT corrections (which by definition contain no basis set superposition er-

TABLE VI. The structure of the dispersion energy for $(H_2O)_2$ in various basis sets. The geometry is the same as in Table V. Energies are given in kcal/mol.

Component	$D(d,p)'$	$D(d,p)^*$	$D(2d,2p)^*$	$T^-(2d,2p)^*$	$T^{-s}(2d,2p)^\dagger$	$D(2df,2pd)^*$
$E_{\rm disp}^{(20)}$	−1.35	−1.57	−1.74	−1.75	−1.70	−1.90
$E_{\rm disp}^{(21)}$	0.02	0.03	0.05	0.05	0.06	0.04
SE[a]	−0.29	−0.32	−0.35	−0.35	−0.34	−0.38
DE[b]	0.31	0.35	0.40	0.40	0.40	0.42
$E_{\rm disp}^{(211)}$	−0.01	−0.01	−0.01	−0.01	−0.01	−0.02
D	−0.00	−0.00	−0.00	−0.00	−0.00	−0.01
Q	−0.01	−0.01	−0.01	−0.01	−0.01	−0.01
$E_{\rm disp}^{(220)}+E_{\rm disp}^{(202)}$	−0.33	−0.34	−0.35	−0.37	−0.36	−0.39
S	−0.17	−0.17	−0.17	−0.18	−0.17	−0.18
D	−0.02	−0.02	−0.02	−0.03	−0.03	−0.03
T	−0.20	−0.23	−0.27	−0.27	−0.27	−0.30
Q	0.06	0.08	0.11	0.11	0.11	0.12
$E_{\rm disp}^{(30)}$	0.00	0.02	0.03	0.03	0.03	0.06

[a] "Single excitation" diagram (the second diagram in Fig. 3).
[b] "Double excitation" diagram (the third diagram in Fig. 3).

TABLE VII. Components of the interaction energy for the water dimer as functions of the angle β. Energies are in kcal/mol, the basis is $T^-(2d,2p)^*$, the monomer's geometry is from Ref. 71, and $\beta = 150°$ corresponds exactly to the geometry given in Table III (see Table V for the notation).

Component$\backslash\beta$	120°	150°	180°
ΔE_{CP}^{SCF}	−3.65	−3.70	−3.47
$E_{pol}^{(10)}$	−7.13	−6.70	−6.28
$E_{exch}^{(10)}$	5.14	4.55	4.29
$E_{pol}^{(12)}$	0.23	0.38	0.39
$E_{ind}^{(20)}$	−1.79	−1.59	−1.50
$E_{disp}^{(20)}$	−1.85	−1.75	−1.71
$E_{exch\text{-}disp}^{(20)}$	0.31	0.27	0.26
$E_{disp}^{(21)}$	0.03	0.05	0.06
$E_{disp}^{(22)}$	−0.42	−0.37	−0.35
$E_{disp}^{(30)}$	0.03	0.03	0.03
$\Delta E_{CP}^{(2)}$	−0.75	−0.66	−0.65
$\Delta E_{CP}^{(3)}$	0.03	0.02	0.03
$\Delta E_{CP}^{(4)}$	−0.01	−0.00	−0.01
$E^{(10)} + E_{ind}^{(20)}$	−3.78	−3.74	−3.49
SAPT	−5.45	−5.13	−4.81
SCF + SAPT	−5.32	−5.09	−4.79
SCF + $MBPT2_{CP}$	−4.40	−4.36	−4.12
SCF + $MBPT4_{CP}$	−4.38	−4.34	−4.10

ror) provides a convincing argument in favor of applying the CP correction at all levels in the supermolecular approach.

Although adding the CP correction obviously leads to much better converging interaction energies, the very large size of this correction at the correlated level even in our largest basis set (the correction is two times larger than the corrected interaction energy itself) is somewhat worrisome. Moreover, the CP approach should be viewed as a method of *partial* removal of the basis set unsaturation error and one may ask how much of this error (e.g., due to unsaturated monomer multipole moments) is left in the CP-corrected energies.

C. Potential energy curves for the water dimer

To investigate the radial dependence of intermolecular interaction energy components, we attempted a limited geometry optimization to find the minimum configuration. There exists a general consensus that the geometry shown in Table III is very close to the minimum one. To determine it more precisely, we first varied the angle β between the O–O axis and the HOH bisector of the proton acceptor. (The coordinates given in Table III correspond to $\beta = 150°$). The results computed in the basis $T^-(2d,2p)^*$ are shown in Table VII. The differences between the values for $\beta = 150°$ given in Table VII and the corresponding ones from Table V result from the slightly different monomer's geometry used in the two calculations. The interaction energy curves exhibit broad minima in this region of β values. A quadratic fit to the SCF + SAPT interaction energies predicts a minimum at $\beta = 85°$. The apparent smallness of this angle results from the neglect of the correlation correction to the valence repulsion in the present implementation of SAPT (see discussion below). This correction is positive and increases with the decrease of β. On the other hand, the SCF + MBPT4 curve has a minimum at $\beta = 130°$. We have therefore decided to compute the potential energy curve as a function of R for an intermediate value of β equal to 120°.

In Table VIII and in Fig. 11, we present the interaction energy components for the water dimer as functions of the O–O separation R in the configuration established above.

TABLE VIII. Components of the interaction energy for the water dimer as functions of the O···O distance R (in Å, 1 Å = 0.529 177 249 bohr, coordinates rounded to five decimal digits), energies are in kcal/mol, the basis is $T^-(2d,2p)^*$, the monomer's geometry is from Ref. 71, and $R = 3.00$ Å corresponds to the geometry given in Table III except that β is equal to 120° (see Table V for notation). All the supermolecular components are with the CP correction included.

Component$\backslash R$	2.50	2.85	2.95	3.00	3.50	4.00	5.00
ΔE_{CP}^{SCF}	2.78	−3.19	−3.57	−3.65	−2.98	−1.96	−0.88
$E_{pol}^{(10)}$	−19.63	−9.37	−7.79	−7.13	−3.41	−1.97	−0.86
$E_{exch}^{(10)}$	30.77	8.83	6.16	5.14	0.83	0.13	0.00
$E_{pol}^{(12)}$	−0.30	0.15	0.21	0.23	0.27	0.21	0.11
$E_{ind}^{(20)}$	−11.35	−3.04	−2.13	−1.79	−0.37	−0.10	−0.02
$E_{disp}^{(20)}$	−5.86	−2.60	−2.07	−1.85	−0.63	−0.24	−0.05
$E_{exch\text{-}disp}^{(20)}$	1.44	0.50	0.36	0.31	0.06	0.01	0.00
$E_{disp}^{(21)}$	0.37	0.07	0.04	0.03	0.00	0.00	0.00
$E_{disp}^{(22)}$	−1.17	−0.56	−0.46	−0.42	−0.16	−0.06	−0.01
$E_{disp}^{(30)}$	0.06	0.04	0.04	0.03	0.01	0.00	0.00
$\Delta E^{(2)}$	−1.76	−1.00	−0.83	−0.75	−0.27	−0.08	0.02
$\Delta E^{(3)}$	0.30	0.06	0.04	0.03	−0.01	−0.01	−0.00
$\Delta E^{(4)}$	−0.05	−0.02	−0.02	−0.01	0.01	0.01	0.02
$E^{(10)} + E_{ind}^{(20)}$	−0.21	−3.58	−3.76	−3.78	−2.95	−1.94	−0.88
$E_{pol}^{(12)} + E_{disp}^{(20)} + E_{exch\text{-}disp}^{(20)}$	−4.72	−1.95	−1.50	−1.31	−0.30	−0.02	0.06
δ	2.96	0.95	0.67	0.56	0.03	−0.06	−0.04
$SAPT_{corr}$	−5.46	−2.40	−1.88	−1.67	−0.45	−0.08	0.05
MBPT4	−1.51	−0.96	−0.81	−0.73	−0.27	−0.08	0.03

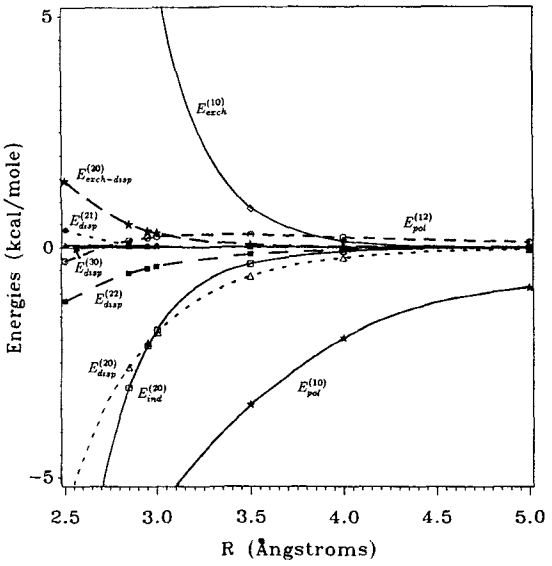

FIG. 11. Components of the many-body SAPT as functions of the intermolecular distance R. The curves are: open stars—$E^{(10)}_{pol}$; diamonds—$E^{(10)}_{exch}$; circles—$E^{(12)}_{pol}$; squares—$E^{(20)}_{ind}$; triangles—$E^{(20)}_{disp}$; full stars—$E^{(20)}_{exch\text{-}disp}$; dots—$E^{(21)}_{disp}$; full squares—$E^{(22)}_{disp}$; full triangles—$E^{(30)}_{disp}$. The configuration is the same as in Table VIII.

All the calculations were performed in the $T^{-}(2d,2p)^{*}$ basis. Table V showed that with this basis set, the individual SAPT energy corrections at the van der Waals minimum should be accurate to at least 0.1 kcal/mol, except for $E^{(20)}_{disp}$ which contains about 0.2 kcal/mol error. Since all these corrections are calculated directly, the relative errors should be the same for other distances. With this estimation, we can discuss the relative importance of various energy corrections. Figure 11 shows the well-known fact that around the minimum the interaction energy consists of four major contributions $E^{(10)}_{pol}$, $E^{(10)}_{exch}$, $E^{(20)}_{ind}$, and $E^{(20)}_{disp}$. Due to its exponential decay, $E^{(10)}_{exch}$ is dominant for smaller distances, but is completely negligible for larger R. $E^{(10)}_{pol}$ dominates at larger distances due to its slow R^{-3} decay. The sum of $E^{(10)}_{pol}$, $E^{(10)}_{exch}$, and $E^{(20)}_{ind}$ reproduces remarkably well the SCF interaction energy ΔE^{SCF}_{CP} over all the distances, revealing the simple physical structure of the latter. This agreement is, however, to some extent fortuitous, resulting from mutual cancellations of higher-order effects included in ΔE^{SCF}_{CP}. Nevertheless, it shows that the simple method of estimating ΔE^{SCF}_{CP} by the sum $E^{(10)}+E^{(20)}_{ind}$ might provide a reasonable approximation, particularly for larger systems.

As mentioned above, $E^{(20)}_{disp}$ dominates the correlated part of the interaction energy around the minimum and for smaller distances. Only at large R the correction $E^{(12)}_{pol}$ becomes more important due to its R^{-3} asymptotic behavior. Because the water molecule has large permanent multipole moments, the $E^{(12)}_{pol}$ correction is actually quite important for all R. Around the minimum, this component is repulsive and dampens about 6% of the electrostatic interaction. For $R=5$ Å, this damping increases to 13%. At small R, $E^{(12)}_{pol}$ changes sign. This behavior can be understood by considering the multipole expansion of this correction. At shorter intermolecular separation, the attractive quadrupole–dipole term proportional to R^{-4} is larger than the repulsive dipole–dipole term. For larger R, the latter term, proportional to R^{-3}, dominates and the entire $E^{(12)}_{pol}$ correction is repulsive. Table VII also shows that $E^{(12)}_{pol}$, as expected, is strongly dependent on the orientation of water molecules.

Among the remaining SAPT corrections contributing to the correlated part of the interaction energy, none is as important at any R as $E^{(20)}_{disp}$ or $E^{(12)}_{pol}$. Two of those remaining corrections $E^{(20)}_{exch\text{-}disp}$ and $E^{(22)}_{disp}$ give significant contributions, while two others, $E^{(21)}_{disp}$ and $E^{(30)}_{disp}$, are almost negligible.

The exchange-dispersion energy $E^{(20)}_{exch\text{-}disp}$ dampens about 10% of the second-order dispersion interaction around the minimum. For larger R, it rapidly becomes unimportant due to its exponential decay.

The smallness of $E^{(21)}_{disp}$ has been discussed already in Sec. V B for the near-equilibrium configuration. Table VIII shows that the same is true for all other distances. On the other hand, the next term in the expansion of the second-order dispersion energy, the $E^{(22)}_{disp}$ correction, gives quite a significant contribution for all R. This correction constitutes about 18% of our total second-order dispersion energy. $E^{(22)}_{disp}$ is also the most time consuming part of our calculations. Its inclusion appears to be important for high-accuracy interaction energies. At the same time, this term can be omitted if one aims at the interaction energies to be accurate to about 10% or less.

The $E^{(30)}_{disp}$ correction is very small, showing that the previous[21–23] estimations of the fast convergence of expansion (2) were correct. From a practical point of view, this component of the interaction energy can be omitted in future calculations for the water dimer and probably for the majority of medium size molecules.

The largest neglected correction in our SAPT expansion is certainly the correlation correction to the first-order exchange energy. We have recently made a first step in the direction of including this correction by computing the two leading terms $E^{(11)}_{exch}$ and $E^{(12)}_{exch}$ for the He_2 system.[40] Work on extension of this method to larger systems is in progress. This correction may be of the order of 10% of $E^{(10)}_{exch}$. Chalasinski and Szczesniak[79] have conjectured that there exists the following relation between $\Delta E^{(2)}$ and the SAPT corrections:

$$\Delta E^{(2)}_{CP} \approx E^{(20)}_{disp} + E^{(12)}_{pol} + E^{(20)}_{exch\text{-}disp} + E^{(11)}_{exch} + E^{(12)}_{exch} + E_{other}, \quad (111)$$

where E_{other} denotes the induction-correlation terms plus some self-consistency (response) and "exchange-deformation" terms. All the components collected in E_{other} are difficult to define in SAPT, but it is assumed that this term is relatively small compared to the corrections explicitly entering Eq. (111). With this assumption, the knowledge of the corrections $\Delta E^{(2)}_{CP}$, $E^{(20)}_{disp}$, $E^{(12)}_{pol}$, and $E^{(20)}_{exch\text{-}disp}$ can be used to estimate the exchange correlation correction to the first-order energy for R around the minimum and smaller

$$\tilde{\varepsilon}^{(1)}_{exch\text{-}corr} \approx \Delta E^{(2)} - E^{(20)}_{disp} - E^{(20)}_{exch\text{-}disp} - E^{(12)}_{pol}. \quad (112)$$

Notice, that the correction $\tilde{\varepsilon}^{(1)}_{exch\text{-}corr}$ must decay exponential-

TABLE IX. Total interaction energies for the water dimer (in kcal/mol) obtained with various methods. Geometries are the same as in Table VIII. All the supermolecular components of the interaction energy are calculated with the CP correction included (see Table V for notation).

Method	2.50	2.85	2.95	3.00	3.50	4.00	5.00
SCF	2.78	−3.19	−3.57	−3.65	−2.98	−1.96	−0.88
SAPT	−5.67	−5.98	−5.64	−5.45	−3.40	−2.02	−0.83
SCF + $E_{disp}^{(20)}$	−3.08	−5.79	−5.64	−5.50	−3.61	−2.20	−0.93
SCF + $E_{disp}^{(20)} + E_{pol}^{(12)}$	−3.39	−5.64	−5.43	−5.27	−3.34	−1.99	−0.82
SCF + SAPT	−2.68	−5.59	−5.45	−5.32	−3.43	−2.04	−0.83
SCF + MBPT2	1.02	−4.19	−4.40	−4.40	−3.25	−2.04	−0.86
SCF + MBPT4	1.27	−4.15	−4.38	−4.38	−3.25	−2.04	−0.85

ly so that the formula (112) cannot be accurate at large R since the right-hand side of Eq. (112) falls off like R^{-n}. Using the ideas of the response (or "relaxed") density theory,[80] Chalasinski and collaborators[81] proposed an improved version of the formula (111), but still the long-range character of the difference between $\Delta E^{(2)}$ and SAPT corrections has not been eliminated. If we tentatively assume that Eq. (111) holds at intermediate separations, the data reported in Table VIII show that at the minimum $\tilde{\varepsilon}_{exch\text{-}corr}^{(1)}$ should be of the order of 0.6 kcal/mol which represents over 10% of $E_{exch}^{(10)}$, similarly as for the He dimer case.[40]

In the last rows of Table VIII, we give the CP-corrected values of the correlation components of the interaction energy obtained using the supermolecular MBPT method. Both the third- and the fourth-order corrections are essentially negligible for all values of R. In addition, for several values of R, the third-order correction almost completely cancels the fourth-order one. Thus, for the water dimer at the investigated configuration, the large numerical effort connected with calculations beyond the second order is not needed. Notice, that this observation would not hold in the CP-uncorrected approach. Similar conclusions can be drawn for the HF dimer, as discussed later. It remains to be seen if the same is true for other configurations and for other molecules. Unfortunately, there are not too many literature calculations of the CP-corrected full fourth-order MBPT energies which use decent quality basis sets.

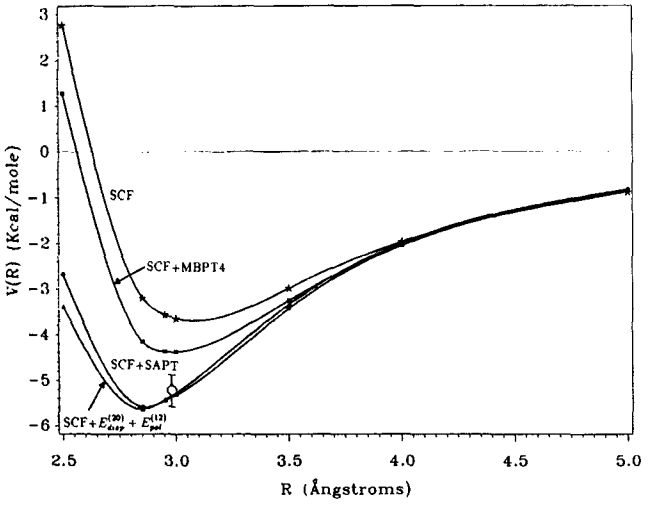

FIG. 12. Total interaction energies obtained with various schemes as functions of the intermolecular distance R. The curves are as follows: stars—SCF; squares—SCF + MBPT4; triangles—SCF + $E_{pol}^{(12)} + E_{disp}^{(20)}$; circles—SCF + SAPT. All the supermolecular components are computed with the CP correction included. The configuration is the same as in Table VIII.

The total interaction energies computed in various approaches are shown as functions of R in Table IX. Some of these energies are plotted in Fig. 12. All the supermolecular energies are computed with the CP correction. The total SAPT interaction energy is very close to the value obtained in the SCF + SAPT approach. This fact is, of course, due to the previously discussed agreement between the SCF interaction energies and the sum of those SAPT corrections which are included in the former energies. In general, we will expect the hybrid SCF + SAPT approach to give a better approximation of the exact interaction energy than the pure SAPT approach since more perturbation-expansion terms are included in the former result via infinite-order summations contained in the SCF supermolecular energies. Table IX also shows the interaction energies for two truncated hybrid methods, i.e., SCF + $E_{disp}^{(20)}$ and SCF + $E_{disp}^{(20)} + E_{pol}^{(12)}$. The former method, sometimes labeled as SCF + DISP, is the simplest possible method of incorporating the electron correlation effects in the interaction energy calculations. The interaction energy calculated using this method is within about 10% or 0.3 kcal/mol of the SCF + SAPT result in the whole range of R. The next method, i.e., SCF + $E_{disp}^{(20)} + E_{pol}^{(12)}$, takes into account the effect of electron correlation on the monomer's electric moments, which improves significantly the agreement with SCF + SAPT for larger R. As discussed above, this method should also improve the angular dependence of the interaction energy. The method is still very simple and applicable for larger chemical systems due to the only $N^4(E_{disp}^{(20)})$ and $N^5(E_{pol}^{(12)})$ dependencies on the number of basis functions N. The SCF + $E_{disp}^{(20)} + E_{pol}^{(12)}$ potential seems in particular to be more suitable than the SCF + $E_{disp}^{(20)}$ potential in studies of hydrogen-bonded systems where the multipole interactions play a major role. At large intermolecular separations, due to the fast decay of $E_{disp}^{(20)}$ compared to $E_{pol}^{(1)}$, the shape of a potential energy surface is determined mainly by the electrostatic components of the interaction energy. The formula SCF + $E_{disp}^{(20)} + E_{pol}^{(12)}$ seems to form an attractive basis for

developing simple analytical potentials describing interactions of polar molecules.

The last two rows of Table IX give the supermolecular interaction energies obtained at the SCF + MBPT2 and SCF + MBPT4 levels of theory, respectively. The potential energy curves computed with these approaches would be almost indistinguishable on the scale of Fig. 12 and lie above the SCF + SAPT curve up to $R = \sim 4$ Å. The improved agreement between the SAPT and MBPT methods for larger R is obviously due to the exponential decay of the first-order exchange-correlation energy. These methods also predict a somewhat larger equilibrium distance of about 2.95 vs 2.85 Å given by the SCF + SAPT approach. If, however, the $\tilde{\varepsilon}^{(1)}_{\text{exch-corr}}$ correction estimated via Eq. (112) is added to the SCF + SAPT energy, the agreement in both the depth and the position of the minimum is significantly improved. The minimum is now only 0.4 kcal/mol below the SCF + MBPT4 result and it is shifted to 2.95 Å. This equilibrium distance is in excellent agreement with the experimental value of 2.98 Å (Ref. 73). All the correlated potential energy curves are probably by about 0.1 kcal/mol too shallow due to omitting the f-symmetry orbitals in the $T^{-}(2d,2p)^{*}$ basis. These orbitals improve the dispersion energy quite significantly (cf. Table V). If this basis set convergence error is added to the results of Table IX, the SCF + SAPT method (corrected by $\tilde{\varepsilon}^{(1)}_{\text{exch-corr}}$) predicts the minimum depth of 4.9 kcal/mol, while the SCF + MBPT4 approach gives 4.5 kcal/mol. The convergence trends of the MBPT4 interaction energy shown in Table V and in Table V of Ref. 10 seem to imply that a further increase of the basis set can only increase the absolute value of this energy. The smallness of the $\Delta E^{(3)}$ and $\Delta E^{(4)}$ corrections, as well as the coupled-cluster calculations of Refs. 10 and 74 [at the coupled-cluster singles, doubles, plus noniterated triples (CCSD-T) level] indicate that the corrections beyond the fourth order are completely negligible for the interaction energy. Therefore, barring unexpected effects resulting from the supermolecular character of the method, the value of -4.5 kcal/mol most likely represents an upper limit of the interaction energy at the minimum. It also seems highly unlikely that the MBPT interaction energy can be lowered by more than 0.4 kcal/mol. Therefore, the SAPT result probably represents the lower limit. It is difficult to say which of the results, the MBPT or the SAPT, provides a more accurate theoretical value of the water dimer interaction energy. Therefore, our final recommendation for the theoretical value of this energy is -4.7 ± 0.2 kcal/mol. This estimate agrees with that of -4.7 ± 0.35 given in Ref. 10 and with a recent estimate -4.7 ± 0.3 of Vos, Hendriks, and van Duijneveldt[82] from MBPT2 calculations in a medium size, interaction energy optimized basis containing functions similar to our $T^{-}(d,p)^{*}$ set plus bond functions. Our value is at the lower limit of the commonly accepted experimental range -5.4 ± 0.7 kcal/mol[83] and may suggest that the experimental estimate from Ref. 84 equal to -5.4 ± 0.2 kcal/mol contains too narrow error bars.

D. Hydrogen fluoride dimer

Our computations for the hydrogen fluoride dimer have been performed for three geometries described in Sec. V A. In Table X, we investigate the basis set convergence of the $(HF)_2$ interaction energy for near equilibrium (nonlinear) geometry. This table shows that all the observations concerning the basis set convergence made for the water dimer remain valid in this case. Some of the discussed features are even more visible now. For example, the CP-uncorrected MBPT interaction energies vary much more dramatically with the basis set, yielding a factor of 3 or a 2.88 kcal/mol difference between the extreme cases. Also, while the CP-corrected MBPT energies vary in a range similar to that for the water dimer, the total MBPT contribution has almost the same absolute value in the smallest and in the largest basis sets, but the sign of it is opposite in the two cases. The necessity of using triple-zeta plus double polarization quality basis sets to correctly predict even the sign of the correlated part of the interaction energy clearly shows the difficulties connected with the use of the supermolecular approach.

In Table XI, we display the components of the interaction energy computed with the $T^{-s}(2df,2pd)^{\dagger}$ basis set for all the investigated geometries of the $(HF)_2$ complex. In all cases, the results are again very similar to those obtained for the water dimer. We only note the relatively larger role of the correlation correction to the electrostatic energy. For the linear attractive geometry, the repulsive $E^{(12)}_{\text{pol}}$ energy, equal to 0.98 kcal/mol, cancels to a large extent the dispersion interaction. For the repulsive geometry, this component is negative and even larger in absolute value than $E^{(20)}_{\text{disp}}$. We do not present the breakup of the $E^{(22)}_{\text{disp}}$ correction into its components. These components are in general similar to those for the water dimer except that for $(HF)_2$ the single-excitation component of $E^{(22)}_{\text{disp}}$ is much larger than the contribution of the double and quadruple excitations and is nearly equal to the contribution given by the triple excitations.

In Table XII, we compare the total interaction energies for $(HF)_2$ obtained using various schemes and our largest $T^{-s}(2df,2pd)^{\dagger}$ basis set. For the equilibrium configuration, the interaction energy obtained in the SCF + SAPT scheme is equal to -4.85 kcal/mol. If this energy is corrected by the estimated value of $\tilde{\varepsilon}^{(1)}_{\text{exch-corr}}$, we obtain 4.4 kcal/mol as the potential depth at minimum. The same depth from the SCF + MBPT4 CP-corrected calculations is 4.0 kcal/mol. Therefore, analogously as for the water dimer, we would estimate the theoretical depth at the minimum to be 4.2 ± 0.2 kcal/mol. Frisch *et al.*[72] computed the SCF + MBPT4 energy using the CP-uncorrected approach only and a basis set somewhat larger than the largest one used by us. Their result of -5.03 kcal/mol is in good agreement with experiment (see the following discussion). This agreement, however, has to be considered as due to accidental cancellation of two errors: the basis set superposition error (BSSE) and the error resulting from using a basis set with energy optimized exponents. Recently, Dayton, Jucks, and Miller[85] measured the dissociation energy of the HF dimer with astonishing accuracy obtaining $D_0 = 3.045 \pm 0.014$ kcal/mol. This value is consistent with the older result of Pine and Howard[86] $D_0 = 2.97^{+0.12}_{-0.10}$ kcal/mol. To obtain the depth at the minimum, we have to add to D_0 the value of the zero-point energy (ZPE). This energy has been computed in Ref. 72 at the MBPT2 level using a

TABLE X. Comparison of the interaction energies for $(HF)_2$ obtained with various schemes and basis sets. The SCF energies are always given with the CP correction included. Nonlinear geometry, energies are in kcal/mol.

Method	$D(d,p)'$	$D(2d,2p)'$	$T^{-S}(2d,2p)^{\dagger}$	$T^{-S}(2df,2pd)^{\dagger}$
SCF	−4.00	−3.74	−3.58	−3.66
$E^{(10)}_{pol}$	−6.99	−6.56	−6.28	−6.33
$E^{(10)}_{exch}$	4.75	4.60	4.56	4.57
$E^{(12)}_{pol}$	0.50	0.43	0.45	0.46
$E^{(20)}_{ind}$	−1.94	−1.93	−1.97	−2.00
$E^{(20)}_{disp}$	−0.97	−1.17	−1.36	−1.49
$E^{(20)}_{exch\text{-}disp}$	0.14	0.18	0.20	0.22
$E^{(21)}_{disp}$	−0.03	0.02	0.01	0.00
$E^{(22)}_{disp}$	−0.30	−0.32	−0.37	−0.41
$E^{(30)}_{disp}$	0.00	0.01	0.02	0.03
$SAPT_{corr}$	−0.66	−0.85	−1.05	−1.19
SAPT	−4.84	−4.74	−4.74	−4.95
$\Delta E^{(2)}_{NCP}$	−1.49	−1.01	−2.41	−2.89
$\Delta E^{(2)}_{CP}$	0.32	−0.03	−0.24	−0.34
$\Delta E^{(3)}_{NCP}$	0.01	0.07	0.05	0.04
$\Delta E^{(3)}_{CP}$	−0.08	−0.03	−0.04	−0.06
$\Delta E^{(4)}_{NCP}$	−0.19	−0.14	−0.01	−0.06
$\Delta E^{(4)}_{CP}$	0.14	0.12	0.08	0.06
$SCF + E^{(20)}_{disp}$	−4.97	−4.91	−4.94	−5.15
$SCF + E^{(20)}_{disp} + E^{(12)}_{pol}$	−4.47	−4.48	−4.49	−4.69
$SCF + SAPT_{corr}$	−4.66	−4.59	−4.63	−4.85
$SCF + MBPT2_{NCP}$	−5.49	−4.75	−5.99	−6.55
$SCF + MBPT2_{CP}$	−3.68	−3.77	−3.82	−4.00
$SCF + MBPT4_{NCP}$	−5.67	−4.82	−6.05	−6.65
$SCF + MBPT4_{CP}$	−3.62	−3.68	−3.78	−4.00

TABLE XI. SCF, many-body SAPT, and supermolecular MBPT interaction energy components for various geometries of the hydrogen fluoride dimer. The basis $T^{-S}(2df,2pd)^{\dagger}$ was used, energies are in kcal/mol (see Table V for notation).

	Geometry		
Component	Repulsive	Attractive	Nonlinear
ΔE^{SCF}_{NCP}	29.22	−4.16	−4.43
ΔE^{SCF}_{CP}	30.78	−3.07	−3.66
$E^{(10)}_{pol}$	27.78	−4.68	−6.33
$E^{(10)}_{exch}$	10.08	3.04	4.57
$E^{(12)}_{pol}$	−3.52	0.98	0.46
$E^{(20)}_{ind}$	−7.05	−1.48	−2.00
$E^{(10)} + E^{(20)}_{ind}$	30.81	−3.12	−3.76
$E^{(20)}_{disp}$	−2.46	−1.28	−1.49
$E^{(20)}_{exch\text{-}disp}$	0.21	0.15	0.22
$E^{(21)}_{disp}$	−0.03	0.04	0.00
$E^{(22)}_{disp}$	−0.66	−0.34	−0.41
$E^{(30)}_{disp}$	0.11	0.02	0.03
$\Delta E^{(2)}_{NCP}$	−7.68	−2.24	−2.89
$\Delta E^{(2)}_{CP}$	−3.58	0.03	−0.34
$\Delta E^{(3)}_{NCP}$	0.14	−0.08	−0.04
$\Delta E^{(3)}_{CP}$	0.11	−0.12	−0.06
$\Delta E^{(4)}_{NCP}$(SDQ)	−0.08	0.17	0.17
$\Delta E^{(4)}_{CP}$(SDQ)	−0.12	0.16	0.15
$\Delta E^{(4)}_{NCP}$(SDTQ)	−1.03	−0.02	−0.06
$\Delta E^{(4)}_{CP}$(SDTQ)	−0.84	0.13	0.06
δ	2.19	0.18	0.47
SAPT	−6.35	−0.43	−1.19
$MBPT4_{CP}$	−4.31	0.04	−0.34

near quadruple-zeta quality isotropic basis plus two sets of polarization functions [basis 6-311 + + G(2*d*,2*p*) in the notation of Ref. 72] and has been found to be equal to 1.9 kcal/mol. No CP correction was included in those calculations. Comparing the values of ZPE computed at lower levels of theory and with smaller basis sets, we observe that this correction is not very sensitive to those factors. Also, a CP-

TABLE XII. Comparison of the total interaction energies obtained with various schemes for the hydrogen fluoride dimer. The supermolecular interaction energies are always with the CP correction included. The basis $T^{-}(2df,2pd)^{\dagger}$ was used, energies are in kcal/mol (see Tables V and VII for notation).

	Geometry		
Method	Repulsive	Attractive	Nonlinear
SCF	30.78	−3.07	−3.66
$E^{(10)} + E^{(20)}_{ind}$	30.81	−3.12	−3.76
SAPT	24.46	−3.55	−4.95
$SCF + E^{(20)}_{disp}$	28.32	−4.33	−5.15
$SCF + E^{(20)}_{disp} + E^{(12)}_{pol}$	24.80	−3.35	−4.69
$SCF + SAPT_{corr}$	24.43	−3.50	−4.85
$SCF + MBPT2_{CP}$	27.19	−3.04	−4.00
$SCF + MBPT4_{CP}$	26.46	−3.03	−4.01

corrected calculation should not change the result significantly since the CP correction to the potential energy surface is relatively constant in the limited region around the minimum which determines ZPE. Thus, it seems very unlikely that the error of ZPE is larger than 0.1 kcal/mol. Adding the ZPE correction to the experimental D_0 gives the minimum depth of 4.9 ± 0.1 kcal/mol. This value, due to its very small error bars, is in significant disagreement with theoretical values, particularly with the SCF + MBPT4 one.

VII. DISCUSSION AND CONCLUSIONS

We have developed and tested an *ab initio* method for calculation of the intermolecular interaction energies for closed-shell systems. The major features of this approach are as follows:

(i) The intermolecular interaction energy, unlike in the traditional supermolecular method, is calculated directly as a sum of well-defined physical contributions. This reveals the physical nature of the intermolecular interaction and the connection between its strength and the properties (both static and dynamic) of the interacting molecules.

(ii) Since the interaction energy is obtained directly (not as a difference of large numbers), it is free from the BSSE plaguing the supermolecular calculations.

(iii) All components of the interaction energy are size extensive, which enables applications to spatially extended polyatomic molecules.

(iv) Different energy corrections exhibit different radial and angular dependencies, which can be examined in great detail from the point of view of achieving state-of-the-art analytical fits in terms of physically interpretable parameters.

(v) Since the individual energy corrections show very different basis set requirements, it is advantageous to calculate them separately with specifically optimized basis sets.

(vi) Although our expressions are similar to those of the supermolecular MBPT, the overall computational effort is smaller than in the standard MBPT calculation of equivalent order since the orbital summation ranges are shorter. This feature follows from the fact that the most time consuming components of SAPT can be computed in the monomer-centered basis set, while the supermolecular approach always requires at least one calculation in the full dimer basis. This enables SAPT applications with larger basis sets and to larger molecules than was previously possible at the correlated *ab initio* level. Our largest application so far was to the interaction of uracil molecule with water and we estimate that calculations for systems with over 100 electrons are feasible at present.

(vii) Since our interaction energy components are included implicitly in the supermolecular MBPT interaction energy of appropriate order, the knowledge of their angular and radial dependence and of basis set requirements is essential for an optimal design and error estimation in the supermolecular calculations.

The numerical results obtained for the water and hydrogen fluoride dimers allow us to examine the performance of SAPT. We see that the majority of the SAPT corrections converge very fast with the size of basis set. The corrections which converge somewhat slower happen to be those which are the easiest to compute, therefore large basis sets can be used to obtain their saturated values. The sum $E^{(10)} + E^{(20)}_{\mathrm{ind}}$ rather accurately reproduces $\Delta E^{\mathrm{SCF}}_{\mathrm{CP}}$ for all the investigated configurations and basis sets. The agreement is much better than one could have anticipated since the neglected SAPT corrections which contribute to $\Delta E^{\mathrm{SCF}}_{\mathrm{CP}}$ are not expected to be entirely negligible. Our computed SAPT or SCF + SAPT interaction energies at the experimental minimum configurations are very close to the experimental values both for $(H_2O)_2$ and $(HF)_2$. This agreement, however, has to be considered fortuitous since our SAPT treatment does not include the intramonomer correlation correction to the first-order exchange energy, which is known to be significant. This correction can be, however, estimated by combining the SAPT and MBPT4 results. After this correction is added, the final SAPT interaction energies at the minimum configurations are further from the experimental values than before, but are still significantly closer to them than those resulting from the CP-corrected supermolecular MBPT4 calculations. The intramonomer correlation correction to the first-order exchange energy is positive and it properly dampens the SAPT potential energy curves which, without this term, tend to predict too short minimum distances.

The numerical results allow us also to draw several conclusions about the supermolecular MBPT approach. First, we confirm earlier observations that the supermolecular interaction energies obtained without the CP correction cannot be trusted. The CP-corrected interaction energies change with the increase of the basis set in a predictable way. In particular, there is a very close relation between the basis set dependence of the SCF and the second-order supermolecular components and the corrections $E^{(10)}_{\mathrm{pol}}$ and $E^{(20)}_{\mathrm{disp}}$, respectively, of SAPT. Unfortunately, the total MBPT4 energies at the minima are very far from the experimental values: by 0.9 kcal/mol for both dimers. This difference means that an MBPT4 approach with a large basis set, like the ones used in the present work, can recover only about 47% and 27% of the correlated part of the interaction energy for $(H_2O)_2$ and $(HF)_2$, respectively. For $(HF)_2$, the disagreement between MBPT4 and experiment is really dramatic due to high experimental accuracy. The reasons for this disagreement are not clear to us. As discussed above, the MBPT4 level of theory seems to be high enough for the higher-order effects to be completely negligible. All the known evidence confirms this opinion. Therefore, the only culprit can be the basis set. The supermolecular results indeed converge rather slowly and one cannot exclude that additions of consecutive angular components to the basis sets will change the supermolecular interaction energy on significant places. At the MBPT4 calculation level, it is not practical—due to the present computer capabilities—to increase the basis sets much beyond those used in the present work, and a modest increase does not change the situation (see Ref. 10). A significant extension of the basis sets is, however, possible in the SAPT approach since the two corrections which converge least rapidly are simple and can be very effectively coded. It is hoped that this approach will shed some light on the problem.

ACKNOWLEDGMENTS

We would like to thank Robert Moszynski for reading and commenting on the manuscript and Hayes Williams for his assistance in modifications of our computer codes. We gratefully acknowledge the use of the IBM 3090/300 computer at the University of Delaware Academic Computing Services. This work was partially supported by the Polish Academy of Sciences within the project No. CPBP 01.12 and by the University of Delaware Research Foundation.

APPENDIX A: EXPANSION OF COMMUTATOR EXPRESSIONS

To illustrate the general method employed by us to expand the commutator expressions appearing in Eqs. (51), (53), (69), (79), and (87)–(90), we present here a detailed derivation of Eq. (56). This equation gives essentially the "vacuum" expectation value of the operator $T_A^\dagger[\Omega_B,T_A]$.

We start by representing all operators in a spin-independent form using the orbital unitary-group generators.[50,51,53] Conventionally these generators are denoted by E^i_j or E_{ij}. Since we distinguish electrons of monomers A and B, we have to introduce two kinds of unitary-group generators A^k_l and B^n_m acting on the coordinates of electrons associated with monomer A and B, respectively. The specific definitions of these operators are

$$A^k_l = a^\dagger_{k+}a_{l+} + a^\dagger_{k-}a_{l-}, \quad B^n_m = b^\dagger_{n+}b_{m+} + b^\dagger_{n-}b_{m-}, \tag{A113}$$

where k^+ and k^- denote the spin orbitals obtained by combining the orbital ψ_k with two orthogonal spin functions α and β.

The one-particle operator Ω_B can now be represented as

$$\Omega_B = \omega^l_k A^k_l, \tag{A114}$$

where ω^l_k will stand in this Appendix for $(\omega_B)^l_k$. Similarly, the one-particle cluster operator S_A has the form $S_A = t^a_r A^r_a$, where t^a_r is given by Eq. (58). The spin-independent form of the intermolecular interaction operator and the S operator are[29]

$$V = v^{lm}_{kn}A^k_l B^n_m + (v_A)^m_n B^n_m + (v_B)^l_k A^k_l + V_0 \tag{A115}$$

and

$$S = t^{ab}_{rs}A^r_a B^s_b, \tag{A116}$$

where $t^{ab}_{rs} = v^{ab}_{rs}/\epsilon^{ab}_{rs}$. The two-particle operators and operators of higher particle rank are expressed via the so-called *orbital replacement operators*,[53,52] denoted usually by $E^{ii'\cdots}_{jj'\cdots}$ and defined recursively in terms of the unitary-group generators E^i_j. In our case, the two-particle orbital replacement operators are defined by

$$A^{kk'}_{ll'} = A^k_l A^{k'}_{l'} - \delta^{k'}_l A^k_{l'}, \quad B^{nn'}_{mm'} = B^n_m B^{n'}_{m'} - \delta^{n'}_m B^n_{m'}. \tag{A117}$$

Similar definitions for higher particle rank operators can be found in Ref. 52. This reference also contains discussion of many useful properties of orbital replacement operators. Here we only mention their invariance under identical permutations of the upper and lower indices and the hermitian symmetry under the interchange of upper and lower indices $(A^{kk'\cdots}_{ll'\cdots})^\dagger = A^{ll'\cdots}_{kk'\cdots}$. The intramonomer correlation operator W_A of Eq. (11) can now be written as

$$W_A = \tfrac{1}{2}v^{ll'}_{kk'}A^{kk'}_{ll'} - \tfrac{1}{2}g^{al}_{ak}A^k_l, \tag{A118}$$

while the first-order cluster operator T_A takes the following form:[52,87]

$$T_A = \tfrac{1}{2}t^{aa'}_{rr'}A^{rr'}_{aa'}, \tag{A119}$$

where the cluster amplitudes $t^{aa'}_{rr'}$ are given by Eq. (57).

Using Eqs. (A114) and (A119) to represent Ω_B and T_A, we can write

$$T_A^\dagger[\Omega_B,T_A] = \tfrac{1}{4}t^{pp'}_{cc'}\omega^l_k t^{aa'}_{rr'}A^{cc'}_{pp'}[A^k_l,A^{rr'}_{aa'}], \tag{A120}$$

where implicit summations over p and p' (c and c') are restricted to virtual (occupied) orbitals of molecule A. The products of the spin orbital replacement operators can be expanded using the multiplication rules, which represent in essence a generalization of Wick's theorem to spin-free quantum chemistry[53,52]

$$A^k_l A^i_j = A^{ki}_{lj} + \delta^i_l A^k_j, \tag{A121}$$

$$A^k_l A^{ii'}_{jj'} = A^{kii'}_{ljj'} + \delta^i_l A^{ki'}_{jj'} + \delta^{i'}_l A^{ik}_{jj'}, \tag{A122}$$

$$\begin{aligned} A^{kk'}_{ll'}A^{ii'}_{jj'} = {} & A^{kk'ii'}_{ll'jj'} + \delta^i_l A^{kk'i'}_{jl'j'} + \delta^{i'}_l A^{kk'i}_{jl'j'} \\ & + \delta^i_{l'}A^{kk'i'}_{ljj'} + \delta^{i'}_{l'}A^{kk'i}_{ljj'} + \delta^i_l\delta^{i'}_{l'}A^{kk'}_{jj'} \\ & + \delta^i_{l'}\delta^{i'}_l A^{kk'}_{jj}, \end{aligned} \tag{A123}$$

where the "contractions" giving rise to the Kronecker deltas can be taken only between the lower indices of the first operator in the product and the upper indices of the second operator.

Applying Eq. (122) to the commutator in Eq. (A120), we obtain

$$\begin{aligned} T_A^\dagger[\Omega_B,T_A] = {} & \tfrac{1}{2}t^{pp'}_{cc'}\omega^r_k t^{aa'}_{rr'}A^{cc'}_{pp'}A^{kr'}_{aa'} \\ & - \tfrac{1}{2}t^{pp'}_{cc'}\omega^l_a t^{aa'}_{rr'}A^{cc'}_{pp'}A^{rr'}_{la'}. \end{aligned} \tag{A124}$$

Note, that the uncontracted terms cancel out in evaluating the commutator and that the two single contractions in Eq. (A122) here give identical contributions due to the invariance of the $t^{aa'}_{rr'}$ amplitudes and $A^{kk'}_{ll'}$ operators under a simultaneous transposition of upper and lower indices.

In further evaluations, only the double contractions in Eq. (A123) must be considered since uncontracted virtual labels will give zero contribution after the vacuum expectation value is taken. The "parallel" and "crossed" double contractions again give identical contributions due to the index symmetry of the amplitudes and operators and we find

$$\begin{aligned} \langle T_A^\dagger[\Omega_B,T_A]\rangle = {} & t^{pr'}_{cc'}\omega^r_p t^{aa'}_{rr'}\langle A^{cc'}_{aa'}\rangle \\ & - t^{rr'}_{cc'}\omega^l_a t^{aa'}_{rr'}\langle A^{cc'}_{la'}\rangle. \end{aligned} \tag{A125}$$

Note that the summation over l is now restricted to occupied orbitals only. It is easy to show that when all labels in $A^{kk'}_{ll'}$ refer to occupied orbitals, then

$$\langle A^{cc'}_{aa'}\rangle = 4\delta^c_a\delta^{c'}_{a'} - 2\delta^c_{a'}\delta^{c'}_a \tag{A126}$$

($\langle A^c_a\rangle = 2\delta^c_a$ and the expression for the vacuum expectation value of a general operator $A^{kk'\cdots}_{ll'\cdots}$ is given in Ref. 52). Using this result and the index symmetry of t amplitudes one obtains

$$\langle T_A^\dagger[\Omega_B,T_A]\rangle = (4t^{pr'}_{aa'} - 2t^{rp}_{aa'})\omega^r_p t^{aa'}_{rr'} - (4t^{rr'}_{ca'} - 2t^{rr'}_{a'c})\omega^c_a t^{aa'}_{rr'}. \quad \text{(A127)}$$

After appropriate change of indices ($r\leftrightarrow r'$, $p\rightarrow r''$, $a\leftrightarrow a'$, $c\rightarrow a''$), the last expression becomes identical with the right-hand side of Eq. (56) expanded according to the definition (59).

Since the operators $A^{kk'\cdots}_{ll'\cdots}$ and $B^{nn'\cdots}_{mm'\cdots}$ commute and since the expectation value of the product $A^{kk'\cdots}_{ll'\cdots}B^{nn'\cdots}_{mm'\cdots}$ factorizes

$$\langle A^{kk'\cdots}_{ll'\cdots}B^{nn'\cdots}_{mm'\cdots}\rangle = \langle A^{kk'\cdots}_{ll'\cdots}\rangle\langle B^{nn'\cdots}_{mm'\cdots}\rangle, \quad \text{(A128)}$$

the general rules used above are also sufficient to expand commutators involving V and S operators and, consequently, all commutators appearing in Secs. III and IV.

APPENDIX B: TRIPLE-EXCITATION CONTRIBUTION TO $E^{(220)}_{\rm disp}$

In this appendix, we present a proof of the formula (98) for the triple-excitation contribution to $E^{(220)}_{\rm disp}$. This proof illustrates a general technique used also to derive Eqs. (80), (91), and (94).

Our starting point here is Eq. (89). As a first step in the proof, we have to represent the operator $\Re_{21}([V,T_A]+[W_A,S])$ in a spin-free form. This is possible because the operator $[V,T_A]+[W_A,S]$ is spin free [see Eqs. (A115), (A116), (A118), and (A119)] and $\Re_{nm}(X)$ is spin free provided that X is spin free. The last fact has been proven in Ref. 88 [the operator $U_2\{\Psi\}$ considered in this reference reduces to $\Re_{20}(X)$ for appropriate choice of Ψ]. The specific form of $\Re_{21}(X)$ is

$$\Re_{21}(X) = \tfrac{1}{2}X^{aa'b}_{rr's}A^{rr'}_{aa'}B^s_b/\epsilon^{aa'b}_{rr's}, \quad \text{(B129)}$$

where

$$X^{aa'b}_{rr's} = \tfrac{1}{12}\langle(2A^{aa'}_{rr'} + A^{a'a}_{rr'})B^b_s X\rangle. \quad \text{(B130)}$$

Analogous formulas for $\Re_{10}(X)$, $\Re_{11}(X)$, and $\Re_{20}(X)$ are

$$\Re_{10}(X) = X^a_r A^r_a/\epsilon^a_r, \quad \Re_{11}(X) = X^{ab}_{rs}A^r_a B^s_b/\epsilon^{ab}_{rs} \quad \text{(B131)}$$

and

$$\Re_{20}(X) = \tfrac{1}{2}X^{aa'}_{rr'}A^{rr'}_{aa'}/\epsilon^{aa'}_{rr'}, \quad \text{(B132)}$$

where

$$X^a_r = \tfrac{1}{2}\langle A^a_r X\rangle, \quad X^{ab}_{rs} = \tfrac{1}{4}\langle A^a_r B^b_s X\rangle \quad \text{(B133)}$$

and

$$X^{aa'}_{rr'} = \tfrac{1}{6}\langle(2A^{aa'}_{rr'} + A^{a'a}_{rr'})X\rangle. \quad \text{(B134)}$$

Note that Eq. (A119) is a direct consequence of Eqs. (B132) and (B134). We shall prove here the latter two equations only since the proof of the remaining ones does not involve any new elements. Actually, since $\Re_{20}(X)$ is a spin-free operator, it can always be represented as a linear combination of the orbital replacement operators $A^{rr'}_{aa'}$. Therefore one only has to prove that the expansion coefficients in Eq. (B132) are indeed given by Eq. (B134). To this end, we equate the spin form [Eq. (34)] with the spin-free form [Eq. (B132)] of $\Re_{20}(X)$ and project the resulting equality with $A^{rr'}_{aa'}$. We then obtain

$$\tfrac{1}{2}\langle A^{rr'}_{aa'}|A^{pp'}_{cc'}\rangle X^{cc'}_{pp'}/\epsilon^{cc'}_{pp'} = \tfrac{1}{4}\langle A^{rr'}_{aa'}|a^{\rho\rho'}_{\alpha\alpha'}\rangle\langle a^{\alpha\alpha'}_{\rho\rho'}X\rangle/\epsilon^{\alpha\alpha'}_{\rho\rho'}. \quad \text{(B135)}$$

The right-hand side of Eq. (B135) equals $\langle A^{rr'}_{aa'}|X\rangle/\epsilon^{aa'}_{rr'}$. This can be seen without any manipulations by observing that the operator between $\langle A^{rr'}_{aa'}$ and $X\rangle$ is essentially a projector on the space containing $A^{rr'}_{aa'}$. When the left-hand side is expanded using the technique of Appendix A, Eq. (B135) reduces to

$$4X^{aa'}_{rr'} - 2X^{aa'}_{r'r} = \langle A^{aa'}_{rr'}X\rangle. \quad \text{(B136)}$$

In deriving Eq. (B136), we employed the fact that the coefficients $X^{aa'}_{rr'}$ have the symmetry property $X^{aa'}_{rr'} = X^{a'a}_{rr'}$ necessary to have them defined uniquely. Performing analogous projection with $A^{r'r}_{aa'}$ gives

$$4X^{aa'}_{r'r} - 2X^{aa'}_{rr'} = \langle A^{aa'}_{r'r}X\rangle. \quad \text{(B137)}$$

Solving Eqs. (B136) and (B137) for $X^{aa'}_{rr'}$ leads to Eq. (134). Similar proof holds for Eq. (B130).

Setting $X=[V,T_A]+[W_A,S]$ and evaluating the right-hand side of Eq. (B130) using the technique of Appendix A shows that after some cancellations $X^{aa'b}_{rr's}$ is identical to the right-hand side of Eq. (99). Thus, in view of Eq. (B129),

$$\Re_{21}([V,T_A]+[W_A,S]) = \tfrac{1}{2}W^{aa'b}_{rr's}A^{rr'}_{aa'}B^s_b/\epsilon^{aa'b}_{rr's}, \quad \text{(B138)}$$

where the coefficients $W^{aa'b}_{rr's}$ are given by Eq. (99).

To complete the proof of Eq. (98), the component $\langle X|\Re_{21}(X)\rangle$ has to be expressed in terms of $W^{aa'b}_{rr's}$. This can be done with the help of the identity

$$\langle X|\Re_{21}(X)\rangle = \langle[F_A+F_B,\Re_{21}(X)]|\Re_{21}(X)\rangle \quad \text{(B139)}$$

resulting easily from definition (34). The operator $[F_A+F_B,\Re_{21}(X)]$ is given by expression (B129) except that the denominators $\epsilon^{aa'b}_{rr's}$ are omitted. Using this fact and Eq. (B139), we can write

$$\langle X|\Re_{21}(X)\rangle = \tfrac{1}{4}X^{pp's'}_{cc'b'}X^{aa'b}_{rr's}\langle A^{cc'}_{pp'}A^{rr'}_{aa'}\rangle\langle B^{b'}_{s'}B^s_b\rangle/\epsilon^{aa'b}_{rr's}, \quad \text{(B140)}$$

where $X^{pp's'}_{cc'b'} = (X^{cc'b'}_{pp's'})^*$. Again using the reduction technique of Appendix A, we find

$$\langle X|\Re_{21}(X)\rangle = (4X^{aa'b}_{rr's} - 2X^{a'ab}_{rr's})X^{rr's}_{aa'b}/\epsilon^{aa'b}_{rr's}. \quad \text{(B141)}$$

After substituting $X=[V,T_A]+[W_A,S]$ and $X^{aa'b}_{rr's} = W^{aa'b}_{rr's}$, the above equation reduces to Eq. (98), i.e., to the expression for $E^{(220)}_{\rm disp}(T)$.

[1] J. H. van Lenthe, J. G. C. M. van Duijneveldt-van de Rijdt, and F. B. van Duijneveldt, Adv. Chem. Phys. **69**, 521 (1987).
[2] G. Chalasinski and M. Gutowski, Chem. Rev. **88**, 943 (1988).
[3] R. J. Bartlett, Annu. Rev. Phys. Chem. **32**, 359 (1981).
[4] S. F. Boys and F. Bernardi, Mol. Phys. **19**, 553 (1970).
[5] M. Gutowski, J. H. van Lenthe, J. Verbeek, F. B. van Duijneveldt, and G. Chalasinski, Chem. Phys. Lett. **124**, 370 (1986).
[6] G. F. H. Diercksen, V. Kellö, and A. J. Sadlej, Chem. Phys. **96**, 59 (1986).
[7] M. M. Szczesniak and S. J. Scheiner, J. Chem. Phys. **84**, 6328 (1986).
[8] J. Sauer, P. Hobza, P. Carski, and R. Zahradnik, Chem. Phys. Lett. **134**, 553 (1987).
[9] G. Chalasinski, D. J. Funk, J. Simons, and W. H. Breckenridge, J. Chem. Phys. **87**, 3569 (1987); G. Chalasinski, R. A. Kendall, and J. Simons, J. Phys. Chem. **91**, 6151 (1987); J. Chem. Phys. **87**, 2965 (1987).
[10] K. Szalewicz, S. J. Cole, W. Kolos, and R. J. Bartlett, J. Chem. Phys. **89**, 3662 (1988).

[11] J. H. van Lenthe and F. B. van Duijneveldt, Chem. Phys. Lett. **143**, 435 (1988).
[12] P. Arrighini, *Intermolecular Forces and their Evaluation by Perturbation Theory* (Springer, Berlin, 1981).
[13] B. Jeziorski and W. Kolos, in *Molecular Interactions*, edited by H. Ratajczak and W. J. Orville-Thomas (Wiley, New York, 1982).
[14] J. O. Hirschfelder, Chem. Phys. Lett. **1**, 325 (1967).
[15] A. van der Avoird, P. E. S. Wormer, F. Mulder, and R. M. Berns, Topics Current Chem. **93**, 1 (1980).
[16] I. G. Kaplan, *Intermolecular Interactions* (Elsevier, Amsterdam, 1987), Chap. 3.
[17] D. M. Chipman, J. Chem. Phys. **66**, 1830 (1977); W. H. Adams and E. E. Polymeropoulos, Phys. Rev. A **17**, 11 (1978); **17**, 18 (1978); **17**, 24 (1978); W. Kutzelnigg, J. Chem. Phys. **73**, 343 (1980); D. J. Klein, Int. J. Quantum Chem. **32**, 377 (1987).
[18] D. M. Chipman, J. D. Bowman, and J. O. Hirschfelder, J. Chem. Phys. **59**, 2830 (1973); D. M. Chipman and J. O. Hirschfelder, *ibid.* **59**, 2838 (1973); **73**, 5164 (1980).
[19] J. N. Murrell and G. Shaw, J. Chem. Phys. **46**, 46 (1967).
[20] J. I. Musher and A. T. Amos, Phys. Rev. **164**, 31 (1967).
[21] G. Chalasinski, B. Jeziorski, and K. Szalewicz, Int. J. Quantum Chem. **11**, 247 (1977).
[22] B. Jeziorski, G. Chalasinski, and K. Szalewicz, Int. J. Quantum Chem. **14**, 271 (1978).
[23] B. Jeziorski, W. A. Schwalm, and K. Szalewicz, J. Chem. Phys. **73**, 6215 (1980).
[24] M. Jeziorska, B. Jeziorski, and J. Cizek, Int. J. Quantum Chem. **32**, 149 (1987).
[25] M. Gutowski, M. Kakol, and L. Piela, Int. J. Quantum Chem. **23**, 1843 (1983).
[26] M. Gutowski and L. Piela, Mol. Phys. **64**, 337 (1988).
[27] G. Chalasinski and B. Jeziorski, Mol. Phys. **32**, 81 (1976).
[28] A. J. Sadlej, Mol. Phys. **39**, 1249 (1980).
[29] S. Rybak, K. Szalewicz, B. Jeziorski, and M. Jaszunski, J. Chem. Phys. **86**, 5652 (1987).
[30] R. Ahlrichs, R. Penco, and G. Scoles, Chem. Phys. **19**, 119 (1977).
[31] K. T. Tang and J. P. Toennies, J. Chem. Phys. **66**, 1496 (1977).
[32] R. Feltgen, J. Chem. Phys. **74**, 1186 (1981).
[33] R. Feltgen, H. Kirst, K. A. Kohler, H. Pauly, and F. Torello, J. Chem. Phys. **76**, 2360 (1982).
[34] K. T. Tang and J. P. Toennies, J. Chem. Phys. **80**, 3726 (1984).
[35] B. Jeziorski, R. Moszynski, S. Rybak, and K. Szalewicz, *Lecture Notes in Chemistry* (Springer, New York, 1989), Vol. 52, p. 65.
[36] B. Jeziorski and W. Kolos, Int. J. Quantum Chem. (Suppl.) **12**, 91 (1977).
[37] K. Szalewicz and B. Jeziorski, Mol. Phys. **38**, 191 (1979).
[38] B. Jeziorski, M. Bulski, and L. Piela, Int. J. Quantum Chem. **10**, 281 (1976).
[39] G. Chalasinski and B. Jeziorski, Theor. Chim. Acta **46**, 277 (1977).
[40] P. Jankowski, B. Jeziorski, S. Rybak, and K. Szalewicz, J. Chem. Phys. **92**, 7441 (1990).
[41] F. Coester, Nucl. Phys. **7**, 421 (1958).
[42] J. Cizek, J. Chem. Phys. **45**, 4256 (1966); Adv. Chem. Phys. **14**, 35 (1969).
[43] J. Paldus and J. Cizek, Adv. Quantum Chem. **9**, 105 (1975).
[44] R. J. Bartlett, J. Phys. Chem. **93**, 1697 (1989).
[45] H. J. Monkhorst, B. Jeziorski, and F. E. Harris, Phys. Rev. A **23**, 1639 (1981).
[46] K. Szalewicz, B. Jeziorski, H. J. Monkhorst, and J. G. Zabolitzky, J. Chem. Phys. **78**, 1420 (1983); **79**, 5543 (1983).
[47] J. Paldus, in *New Horizons of Quantum Chemistry*, edited by P.-O. Löwdin and B. Pullman (Reidel, Dordrecht, 1983), p. 31.
[48] F. E. Harris, B. Jeziorski, and H. J. Monkhorst, Phys. Rev. A **23**, 1632 (1981).
[49] B. Jeziorski and H. J. Monkhorst, Phys. Rev. A **24**, 1668 (1981).
[50] J. Paldus, in *Theoretical Chemistry: Advances and Perspectives*, edited by H. Eyring and D. Henderson (Academic, New York, 1976), Vol. 2, p. 131.
[51] F. A. Matsen, Adv. Quantum Chem. **11**, 223 (1978).
[52] J. Paldus and B. Jeziorski, Theor. Chim. Acta **73**, 81 (1988).
[53] W. Kutzelnigg, J. Chem. Phys. **80**, 822 (1984); **82**, 4166 (1985).
[54] B. H. Brandow, Adv. Quantum Chem. **10**, 187 (1977).
[55] S. Kucharski and R. J. Bartlett, Adv. Quant. Chem. **18**, 281 (1986).
[56] M. V. Basilevsky and M. M. Berenfeld, Int. J. Quantum Chem. **6**, 23 (1972).
[57] B. Jeziorski and M. C. van Hemert, Mol. Phys. **31**, 713 (1976).
[58] F. Visser, P. E. S. Wormer, and P. Stam, J. Chem. Phys. **79**, 4973 (1983).
[59] W. Rijks and P. E. S. Wormer, J. Chem. Phys. **88**, 5704 (1988).
[60] A. J. Sadlej, J. Chem. Phys. **75**, 320 (1981); T. C. Caves and M. Karplus, *ibid.* **50**, 3649 (1969); E. A. Salter, H. Sekino, and R. J. Bartlett, *ibid.* **87**, 502 (1987).
[61] V. Kvasnicka, Mol. Phys. **39**, 143 (1980).
[62] M. J. Frisch, J. S. Binkley, H. B. Schlegel, K. Raghavachari, C. F. Melius, R. L. Martin, J. J. P. Stewart, F. W. Bobrowicz, C. M. Rohlfing, L. R. Kahn, D. J. DeFrees, R. Seeger, R. A. Whiteside, D. J. Fox, E. M. Fluder, and J. A. Pople, *Gaussian 86* (Carnegie-Mellon Quantum Chemistry, Pittsburgh, 1984).
[63] T. H. Dunning, J. Chem. Phys. **53**, 2823 (1970).
[64] S. Huzinaga, J. Chem. Phys. **42**, 1293 (1965).
[65] A. J. Sadlej, Coll. Czech. Chem. Commun. **53**, 1995 (1988).
[66] F. B. van Duijneveldt, IBM Research Report, RJ945, 1971.
[67] J. G. C. M. van Duijneveldt-van de Rijdt and F. B. van Duijneveldt, J. Mol. Struct. (Theochem.) **89**, 185 (1982).
[68] L. M. J. Kroon-Batenburg and F. B. van Duijneveldt, J. Mol. Struct. (Theochem.) **121**, 185 (1985); J. Phys. Chem. **90**, 5431 (1986).
[69] M. Jaszunski and B. O. Roos, Mol. Phys. **52**, 1209 (1984); B. O. Roos and A. J. Sadlej, Chem. Phys. **94**, 43 (1985).
[70] G. H. F. Diercksen and A. J. Sadlej, Theor. Chim. Acta **63**, 69 (1983).
[71] G. H. F. Diercksen and A. J. Sadlej, J. Chem. Phys. **75**, 1253 (1981).
[72] M. J. Frisch, J. E. Del Bene, J. S. Binkley, and H. F. Schaefer III, J. Chem. Phys. **84**, 2279 (1986).
[73] B. J. Howard, T. R. Dyke, and W. Klemperer, J. Chem. Phys. **81**, 5417 (1984).
[74] R. J. Harrison and R. J. Bartlett, Int. J. Quantum Chem. Symp. **20**, 437 (1986).
[75] O. Hess, M. Caffarel, C. Huiszoon, and P. Claverie, J. Chem. Phys. **92**, 6049 (1990).
[76] G. Chalasinski, B. Jeziorski, J. Andzelm, and K. Szalewicz, Mol. Phys. **33**, 971 (1977).
[77] M. Gutowski, G. Chalasinski, and J. G. C. M van Duijneveldt-van de Rijdt, Int. J. Quantum Chem. **26**, 971 (1984).
[78] G. Chalasinski and M. Gutowksi, Mol. Phys. **54**, 1173 (1985).
[79] G. Chalasinski and M. M. Szczesniak, Mol. Phys. **63**, 205 (1988).
[80] E. A. Salter, G. W. Trucks, and R. J. Bartlett, J. Chem. Phys. **90**, 1752 (1989); E. A. Salter, G. W. Trucks, G. Fitzgerald, and R. J. Bartlett, Chem. Phys. Lett. **141**, 61 (1987); G. W. Trucks, E. A. Salter, C. Sosa, and R. J. Bartlett, *ibid.* **147**, 359 (1988).
[81] R. Moszynski, S. Rybak, S. M. Cybulski, and G. Chalasinski, Chem. Phys. Lett. **166**, 609 (1990); S. M. Cybulski, G. Chalasinski, and R. Moszynski, J. Chem. Phys. **92**, 4357 (1990).
[82] R. J. Vos, R. Hendriks, and F. B. van Duijneveldt, J. Comp. Chem. **11**, 1 (1990).
[83] L. A. Curtiss, D. J. Frurip, and M. Blander, J. Chem. Phys. **71**, 2703 (1979).
[84] J. Reimers, R. Watts, and M. Klein, Chem. Phys. **64**, 95 (1982).
[85] D. C. Dayton, K. W. Jucks, and R. E. Miller, J. Chem. Phys. **90**, 2631 (1989).
[86] A. S. Pine and B. J. Howard, J. Chem. Phys. **84**, 590 (1986).
[87] B. Jeziorski and J. Paldus, J. Chem. Phys. **88**, 5673 (1988).
[88] B. Jeziorski, H. J. Monkhorst, K. Szalewicz, and J. G. Zabolitzky, J. Chem. Phys. **81**, 368 (1984).